



Multi-year CO₂ budgets in South African semi-arid Karoo ecosystems under different grazing intensities

Oksana Rybchak¹, Justin du Toit², Jean-Pierre Delorme¹, Jens-Kristian Jüdt¹, Kanisios Mukwashi¹, Christian Thau³, Gregor Feig^{4,5}, Mari Bieri¹, Christian Brümmer¹

5 ¹Thünen Institute of Climate-Smart Agriculture, Braunschweig, 38116, Germany

²Grootfontein Agricultural Development Institute, Middelburg, 5900, South Africa

³Department of Earth Observation, Friedrich-Schiller University Jena, Grietgasse 6, 07743 Jena, Germany

⁴South African Environmental Observation Network, Colbyn, Pretoria, 0083, South Africa

⁵Department of Geography, Geoinformatics and Meteorology, University of Pretoria, Pretoria, 0002, South Africa

10

Correspondence to: Oksana Rybchak (oksana.rybchak@thuenen.de), Christian Brümmer (christian.bruemmer@thuenen.de)

Abstract. Climatic and land management factors, such as water availability and grazing intensity, play an important role in seasonal and annual variability of the ecosystem–atmosphere exchange of CO₂ in semi-arid ecosystems. However, the semi-arid South African ecosystems have been poorly studied. Four years of measurements (November 2015–October 2019) were collected and analysed from two eddy covariance towers near Middelburg in the Karoo, Eastern Cape, South Africa. We studied the impact of grazing intensity on the CO₂ exchange by comparing seasonal and interannual CO₂ fluxes for two sites with almost identical climatic conditions but different intensity of current and historical livestock grazing. The first site represents lenient grazing (LG) and the vegetation comprises a diverse balance of dwarf shrubs and grasses, while the second site has been degraded through heavy grazing (HG) in the past but then rested for the past 10 years and mainly consists of unpalatable grasses and ephemeral species. Over the observation period, we found that the LG site was a considerable carbon source (82.11 g C m⁻²), while the HG site was a slight carbon sink (−36.43 g C m⁻²). The annual carbon budgets ranged from −90 ± 51 g C m⁻² yr⁻¹ to 84 ± 43 g C m⁻² yr⁻¹ for the LG site and from −92 ± 66 g C m⁻² yr⁻¹ to 59 ± 46 g C m⁻² yr⁻¹ for the heavily grazed site over the four years of eddy covariance measurements. The significant variation in carbon sequestration rates between the last two years of measurement was explained by water availability (25 % of the precipitation deficit in 2019 compared to the long-term mean precipitation). This indicates that studied ecosystems can quickly switch from a considerable carbon sink to a considerable carbon source ecosystem. Our study shows that the CO₂ dynamics in the Karoo are largely driven by water availability and the current and historical effects of livestock grazing intensity on aboveground biomass (AGB). The higher carbon uptake at the HG site indicates that resting period after overgrazing, together with the transition to unpalatable drought-tolerant grass species, creates conditions that are favourable for carbon sequestration in the Karoo ecosystems, but unproductive as Dorper sheep pasture. Furthermore, we observed a slight decrease in carbon uptake peaks at the HG site in response to resuming continuous grazing (July 2017).

20
25
30



1 Introduction

Global environmental changes (such as global warming, land degradation, etc.) alter ecosystem processes such as photosynthesis, respiration and decomposition, therefore affecting the carbon cycle (Cao et al., 2001; Groendahl et al., 2007; Jung et al., 2017; Miranda et al., 2011; Müller et al., 2007; Yi et al., 2012). Assessment of carbon uptake or release has turned into one of the most critical issues in environmental science in the last decade (Araújo et al., 2002; Ardö et al., 2008; K'Otuto et al., 2013; Nakano and Shinoda, 2018). Even though numerous studies on ecosystem carbon budget have been conducted, most of them have concentrated on European, Asian or North American mid-latitude ecosystems (Anthoni et al., 2004; Bao et al., 2019; Béziat et al., 2009; Fei et al., 2017; Nagy et al., 2006; Niu et al., 2020; Rannik et al., 2002; Rogiers, 2005; Schmid, 2002; Wang et al., 2016; Yan et al., 2017), while a lack of attention has been given to the African continent. Even though South Africa has been heavily affected by climate change during the recent decades (Hulme et al., 2001; Ziervogel et al., 2014), many gaps remain in the understanding of the semi-arid ecosystem carbon exchange (Archibald et al., 2009; Kutsch et al., 2008; Räsänen et al., 2017; Talore et al., 2016; Veenendaal et al., 2004).

Semi-arid ecosystems contribute up to 20 % of terrestrial net primary productivity and are thus of particular concern for the global carbon balance (Ahlström et al., 2015; Meza et al., 2018). By partitioning terrestrial CO₂ among land cover classes, Ahlström et al. (2015) showed that the interannual variability of the net biome production is dominated (39 %) by semi-arid ecosystems. The strong diurnal, seasonal and interannual variability in CO₂ fluxes indicates that carbon exchange can be affected by the ecosystem's response to land management and meteorological forcing (Archibald et al., 2009; Brümmer et al., 2008; Merbold et al., 2009; Nakano and Shinoda, 2018; Räsänen et al., 2016; Sorokin et al., 2017).

Previous studies determined water availability as the main driver controlling gross primary production (GPP) through increasing photosynthesis and extending the length of the growing season (Ago et al., 2016; Bao et al., 2019; Meza et al., 2018; Otieno et al., 2010; Wang et al., 2019). However, the seasonal responses of GPP and ecosystem respiration (R_{eco}) to precipitation pattern and the impacts of precipitation on the annual carbon budget are less well understood in the South African semi-arid ecosystems. These ecosystems are highly seasonal with large parts of total annual precipitation occurring in only a few months of the year, and generally reveal pulse-driven evapotranspiration events in the rainy season. Phase and amplitude of photosynthesis and respiration are also highly dependent on the precipitation pattern (Archibald et al., 2009; Bao et al., 2019; Kutsch et al., 2008; Merbold et al., 2009; Räsänen et al., 2017). The strength of the ecosystem response to rainfall is not only determined by the amount of an individual event, but also on the timing of preceding events (Huxman et al., 2004; Ivans et al., 2006; Veenendaal et al., 2004; Williams et al., 2009; Yepez and Williams, 2009).

Land and vegetation degradation belong to the crucial drivers altering ecosystem–atmosphere carbon exchange. Even though many studies suggest that overgrazing leads to biodiversity losses and soil degradation (Hansis et al., 2015; Kairis et al., 2015), its impact on the ecosystem CO₂ exchange is still not well understood as ecosystems may respond differently depending on their grazing history as well as biotic (vegetation cover) and micrometeorological factors (Chen et al., 2014; Gourlez de la Motte et al., 2018; Müller et al., 2007; Richter and Houghton, 2011; Talore et al., 2016; du Toit et al., 2011; Wang et al., 2019).

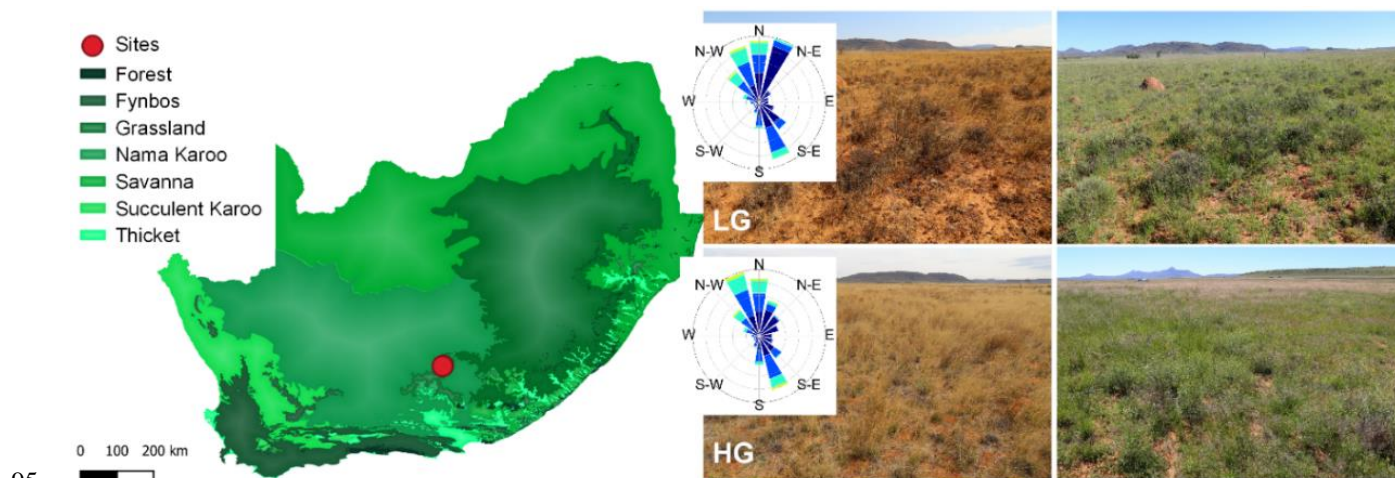


65 Most studies providing comparisons of carbon exchange under different grazing intensities are of short duration, hence they
do not detect seasonal nor annual changes in the carbon dynamics associated with grazing, and are not based on South African
semi-arid ecosystems (Chen et al., 2014; Chimner and Welker, 2011; Frank, 2002; Lecain et al., 2000; Wang et al., 2016; Yan
et al., 2017). Assessing the impacts of livestock grazing on the ecosystem carbon exchange and vegetation cover is important
for understanding the driving factors of carbon dynamics in the semi-arid grazed ecosystems. According to Reyers et al. (2009),
70 about 52 % of the semi-arid Karoo has been moderately or severely degraded due to livestock overgrazing. However, Hoffman
et al. 2018 showed that the situation has improved somewhat at Nama-Karoo for example, by reduction in the number of sheep
from 11 million (1939) to 4 million (2007), and by extension of the protected area (from 0.03 % to 1.6 %).
In this study, we investigated the combined impacts of livestock grazing and the interannual climatic (precipitation) variability
on the ecosystem–atmosphere CO₂ exchange. The study is based on four years of continuous eddy covariance (EC)
75 measurements of CO₂ at semi-arid Karoo near Middelburg, Eastern Cape, South Africa. Our paired-tower approach allowed
for an analysis of the effects of different grazing regimes on CO₂ fluxes under identical climate. The two study sites represent
lenient temporary (LG) vs. continuous heavy grazing (HG). We hypothesize that the HG regime reduces the ecosystem carbon
sink potential by altering vegetation cover, decreasing above-ground biomass (AGB) and gross primary production. In our
analysis we attribute the difference in CO₂ exchange between the two sites to current and historic grazing intensity, while
80 changes in yearly CO₂ budgets are mainly explained by inter-annual variability of rainfall sums and distribution.

2 Methodology

2.1 Sites description

The two study sites were located at an altitude of 1310 m.a.s.l. in the Eastern Upper Karoo vegetation type in the Nama-Karoo,
a biome that occupies much of the central to western inland region of South Africa (Mucina et al., 2006) (Fig. 1). The
85 vegetation is co-dominated by dwarf shrubs (perennial, both succulent and non-succulent) and grasses (short-lived and
perennial), with shrubs, geophytes, sedges and herbs also present. The soils are loamy at both study sites (Roux, 1993; du Toit
and O'Connor, 2020). The climate is characterised by long hot summers and moderate to warm winters (du Toit and O'Connor,
2014). During the summer months, days are generally hot (30–40 °C) and nights are moderately warm (10–16 °C), while the
winter days are moderate to warm (14–25 °C) and nights are cold (–4–4 °C). The long-term mean annual temperature was 15
90 °C. Cool seasons (April–September) and warm seasons (October–March) can be distinguished throughout all years. Mean
annual precipitation was 374 mm from 1889 to 2013 in the range from 163 mm to 749 mm (du Toit et al., 2015).



95

Figure 1. South African biomes and location of the studied sites marked as a red circle with footprints, wind roses on the right side and pictures in dry and growing seasons for the lenient grazing (LG) site (top) and the heavy grazing (HG) site (bottom) (Department of Agriculture Fisheries and Forestry, 2013).

The Lenient Grazing (LG) (31°25'20.97" S, 25°1'46.38" E) site has been grazed by sheep and cattle using a rotational grazing system (approximately 2 weeks grazing followed by 24–26 weeks rest) at recommended stocking rates of 16 hectares per animal unit (ha AU⁻¹) since the 1970s, and is considered to be an excellent condition ‘benchmark’ site in terms of botanical composition, with a wide diversity of species and co-dominance of grasses and dwarf-shrubs (du Toit, 2002). Dominant species are *Digitaria eriantha* (palatable perennial grass) and *Pentzia globosa* (palatable non-succulent dwarf-shrub) (du Toit and Nengwenani, 2019). The Heavy Grazing (HG) (31°25'48.69" S, 25°0'57.70" E) site was grazed by Dorper sheep using a 2-paddock rotational grazing system (120 days grazing followed by 120 days rest) at stocking rates approximately double that of the recommended rate as part of an experimental trial from 1988 to 2007. The Dorper breed is described as a hardy sheep that prefers shrubs to a greater extent than grasses (Brand, 2000). The site was ungrazed 2008–2017 but did not recover, after which Dorpers were reintroduced at a similar stocking rate in July 2017, and the veld was grazed continuously unless (for short periods) food availability was too low. This severe treatment extirpated nearly all palatable species and nearly all dwarf shrubs, and as a result, the system is dominated by *Aristida diffusa* (unpalatable perennial grass) and *Aristida congesta* (short-lived unproductive grass) (van Lingen, 2018). Thus, the HG site is a degraded site from an agricultural point of view, having shifted from a diverse grassy shrubland to unpalatable arid grassland. Climatic conditions of the two sites are similar. There is no information on the difference between the sites in bulk density, soil nitrogen and organic carbon content.

2.2 Instrumentation and measurements

Eddy Covariance (EC) towers were installed at the LG and HG sites to measure ecosystem–atmosphere exchange of carbon, water and heat fluxes in October 2015. The two towers are placed approximately 1.5 km apart. Wind components were measured with a three-dimensional sonic anemometer (CSAT3, Campbell Scientific Inc., Logan, UT, USA) placed 3 m above



the ground. The sonic anemometer was coupled with an enclosed path fast-response Infra-Red Gas Analyser (IRGA) Li-7200 (IRGA, Li-Cor, Lincoln, NE, USA) for CO₂ and H₂O measurements. Air from close proximity (~5 cm) to the sonic
120 anemometer's array was pulled through a sampling tube into the IRGA through a stainless steel tube of 70 cm length and 6.0 mm inner diameter using the pump from Licor's Li-7200-101 Flow Module with a flow rate of 15 L min⁻¹. The IRGA acquisition system collected raw data in real-time at 20 Hz sampling rate, compressed files (meta, flux and biomet data) for later processing. The gas analysers were manually calibrated every six months using standard air calibration tanks with mixing ratios of zero and span (431.23 ppm). Drift of the sensors was always below 1%.

125 Relative humidity and air temperature were recorded with Temperature/Humidity Probe (HMP155, Vaisala, Helsinki, Finland), precipitation with Tipping Bucket Rain Gauge (TR 525, Texas Electronics, Texas, USA), radiation components with Net Radiometer (CNR4, Kipp&Zonen, Delft, Netherlands). Soil measurements consisted of heat flux plates (HFP01 + HFP01 SC, Campbell scientific, Utah, USA) at two different depths (10 and 20 cm) with three repetitions, soil temperature probes (UMS TH3 sdi12, Meter AG, Munich, Germany) at six different depths (5, 6, 10, 13, 20 and 37 cm at LG site and at 10, 12,
130 17, 22, 32 and 57 cm at HG site), soil moisture probe (ML3x Delta T, EcoTech, Bonn, Germany) at two different depths (10 and 16 cm at the LG site and at 8 and 14 cm at the HG site). The two sites differed in soil heterogeneity and characteristics particularly in stone content (soil skeleton >2 mm for the HG site), which were the reasons for different installation depths of the soil temperature and moisture probes.

Also, with the EC installation, we were able to evaluate latent and sensible heat fluxes, energy balance closure, and diurnal
135 variation of the residual of the energy balance. Figures dealing with energy flux topics are briefly described in the Appendix A (Figs. A1, A2, A3, Table A1).

2.3 Data processing

2.3.1 Eddy covariance post-field data processing

Fluxes were calculated on the basis of the EC technique from raw high-frequency data with a half-hourly averaging period,
140 discussed and explained in detail in previous studies (Aubinet et al., 2000; Baldocchi et al., 2001; Burba, 2013; Foken and Wichura, 1996; Moncrieff et al., 1997; Webb et al., 1980) strictly following the recently published processing chain of the FLUXNET methodology by Pastorello et al. (2020). Processing was performed with the EddyPro software package version 7.0.6 to quantify ecosystem-atmosphere exchange of CO₂, water vapour, and sensible heat fluxes. Flux data were available for the four hydrological years from November 2015 to October 2019. Complete datasets consist of 70,129 30-min flux
145 measurements with 8 % for LG site and 12 % for HG site missing data due to instrument failure. After processing, the gaps increased to 12 % and 26 % of the missing data for LG and HG sites, correspondingly.

The absolute limits assessment was performed to filter out implausible data by setting upper and lower thresholds (Aubinet et al., 2000; Baldocchi, 2003; Foken and Wichura, 1996). Spikes were removed by applying the median absolute deviation (MAD) filter (Mauder et al., 2013). The amplitude resolution test to identify data with a low variance was performed according



150 to Vickers and Mahrt (1997). The vertical and horizontal velocity components were transformed to zero to adjust wind
statistics for the misalignment of the sonic anemometer by performing a two-dimensional coordinate system rotation (Aubinet
et al., 2000; Baldocchi et al., 1988; Wilczak et al., 2001). The time lag compensation between the anemometric and gas analyser
variables was detected using the maximum covariance method (Fan et al., 1990). Linear detrending was used to extract
turbulent fluctuations from time-series data (Gash and Culf, 1996). Also, fluxes were corrected following systematic losses in
155 the low and high frequency range due to the data processing choices, system characteristics and sampling ranges of the
instruments (Moncrieff et al., 1997, 2006). Quality control flags were calculated for all fluxes by the flagging methodology
after Foken et al. (2006) and Mauder and Foken (2011). After application of all the correction procedures, half-hourly values
of CO₂, latent and sensible heat fluxes were calculated.

2.3.2 Flux filtering and quality control

160 Based on the criteria after Mauder and Foken (2011), bad quality flux data that obtained the value “2” were discarded from
further analyses. In total, after the quality checking and quality flags filtering procedures, the missing CO₂ flux measurements
data increased to 27 % for the LG site and 34 % for the HG site.

Numerous studies indicate reduced reliability of the nighttime flux measurements due to periods with low turbulent mixing of
the planetary boundary layer (Aubinet et al., 2000; Gu et al., 2005; Twine et al., 2000). Many authors describe a threshold
165 value for the friction velocity (u_*) filtering criterion to remove periods of intermittent turbulence as the EC assumptions fail
during low turbulence periods (Aubinet et al., 2000, 2012; Baldocchi, 2003; Goulden et al., 1996). To identify insufficient
turbulent mixing, we estimated the minimum friction velocity u_* according to the method described in Papale et al. (2006).
Threshold values of u_* were 0.10 m s⁻¹ for both sites. The corrected fluxes were filtered by removing data below these
thresholds from the dataset. After u_* filtering application, the missing CO₂ fluxes data increased to 44 % and 49 % for the LG
170 and HG site, respectively.

After the standard quality assessment and quality control, flux data sets were again checked and filtered for implausible values.
There were a few longer periods of setup malfunction, most of which related to solar panel outages and battery or pump
failures, that lasted for 31 days (10/06/2016–10/07/2016) and 30 days (02/01/2018–31/01/2018) on the LG site and for 33 days
(23/11/2017–15/12/2017) and 104 days (03/02/2018–17/05/2018) on the HG site.

175 2.3.3 Data gap-filling and flux partitioning

The gaps due to the precipitation, non-turbulence conditions, spikes and power breakdowns resulted in 29,641 and 35,942 of
30-min flux gaps for LG and HG sites, respectively. These gaps were filled to obtain continuous dataset for the calculations
of the net CO₂ balance and its component fluxes GPP and R_{eco}.

CO₂ fluxes were gap-filled and GPP and R_{eco} were derived using the gap-filling and flux partitioning REddyProcWeb online
180 tool. The detailed explanation of the gap-filling and partitioning methods are described by Wutzler et al. (2018). The marginal
distribution sampling (MDS) method after Reichstein et al., (2005) is implemented into the tool, which integrates the



covariation of the fluxes with the micrometeorological conditions within a moving time window and the temporal fluxes' autocorrelation based on look-up tables (LUT) and the mean diurnal course (MDC) method (Falge et al., 2001; Wutzler et al., 2018).

185 The main components of the carbon fluxes (GPP and R_{eco}) can be derived by two methods: the so-called nighttime approach by Reichstein et al. (2005) and the daytime approach by Lasslop et al. (2010). Both approaches were tested extensively for ecosystems mainly in the mid-latitudes but less for highly seasonal ecosystems. In the current study, we used the nighttime approach from Reichstein et al. (2005) with the algorithm fitting a respiration model to the measured nighttime CO_2 fluxes data and extrapolating it to daytime data using the corresponding temperature measurements.

190 **2.3.4 Uncertainty estimation**

Flux measurements by EC method are subject to errors, and estimating them is an important criterion for analysing annual net ecosystem exchange (NEE) balances. The annual NEE uncertainty was calculated by taking into account the most significant possible error sources (Finkelstein and Sims, 2001; Lucas-Moffat et al., 2018; Massman and Lee, 2002; Moffat et al., 2007; Richardson et al., 2012): (1) systematic errors associated with advection, flux divergence and tilt correction, (2) random errors associated with inadequate sample size, and (3) bias errors due to the gap-filling of the unavoidable gaps in the EC data sets. 195 associated with inadequate sample size, and (3) bias errors due to the gap-filling of the unavoidable gaps in the EC data sets. The NEE uncertainty estimation equations are described in detail by Moffat et al. (2007) and Lucas-Moffat et al. (2018).

The bias errors resulting from gap-filling of the flux measurement data is provided by the formula:

$$\delta ASum = Np \cdot BE, \quad (1)$$

where $\delta ASum$ is the offset on the annual sum, Np is the number of gap-filled days and BE is the bias error. Moffat et al. (2007) 200 demonstrate that the effect of different gap-filling techniques on the bias error of the annual balance of NEE for their selection of sites was less than $0.25 \text{ g C m}^{-2} \text{ d}^{-1}$.

The random error (RE) was calculated for each 30 minutes flux measurements by EddyPro software using Finkelstein et al. (2001) method. The random error of the annual sum ($\varepsilon ASum$) is calculated by the formula:

$$\varepsilon ASum = \sqrt{\sum RE}, \quad (2)$$

205 Both equations were summed up to estimate total NEE uncertainty for the year:

$$NEE_{total_uncertainty} = \Delta ASum + \varepsilon ASum. \quad (3)$$

2.4 Remote sensing-based NDVI index

Remote sensing-based vegetation indices (VIs) were used to put the observed flux tower measurements into the context of plant functioning and responses to environmental conditions and management. To this end, Moderate Resolution Imaging 210 Spectroradiometer (MODIS) time series provided by the Terra and Aqua satellites were acquired for the period under investigation. More specifically, the MODIS VI products MOD13Q1 (Terra) and MYD13Q1 (Aqua) were downloaded from the National Aeronautics and Space Administration (NASA) Distributed Active Archive Centre (DAAC,



https://ladsweb.modaps.eosdis.nasa.gov/search/). Subsequently, the VI values contained in these products were extracted for the two flux tower locations and compared to the EC measurements.

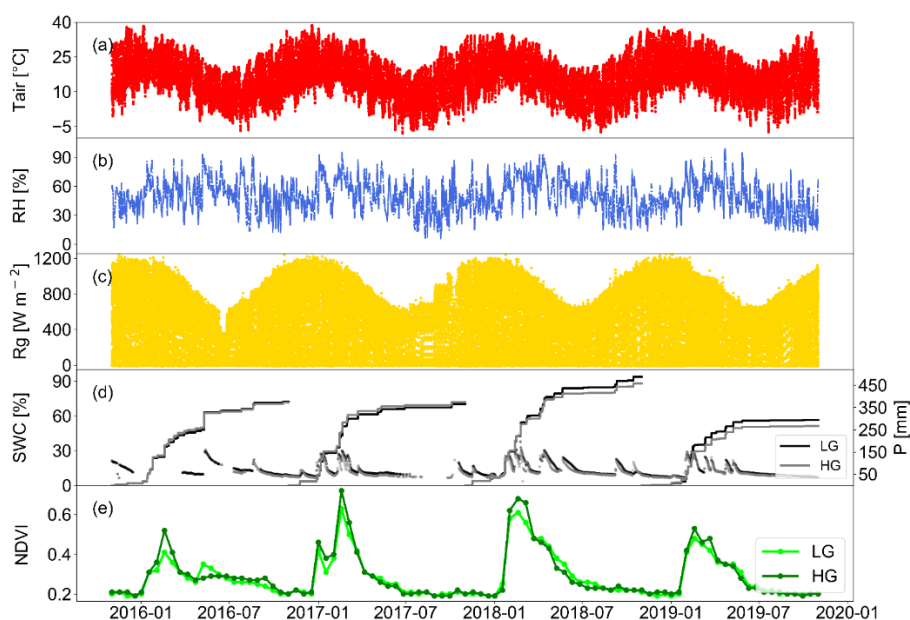
215 Both MOD13Q1 and MYD13Q1 are global data sets featuring a spatial resolution of 250 m and a temporal resolution of 16 days. The VIs that come with the product as a normalized difference vegetation index (NDVI). The NDVI allows for consistent spatio-temporal comparisons of vegetation canopy greenness and canopy structure. The most recent version (collection 6) of MOD13Q1 and MYD13Q1 was employed in this study. For more information, the reader is referred to the products' user guide (Didan et al., 2015) and their algorithm theoretical basis document (ATBD) (Huete et al., 1999).

220 3. Results

3.1. Meteorological conditions

The measured daily and seasonal variability in the main climatic conditions (air temperature, radiation, relative humidity) were typical for the Nama Karoo biome (Fig. 2). We analysed wet (January–May) and dry (June–December) seasons and defined the following periods as hydrological years (HY):

- 225
- Year I (01/11/2015 – 31/10/2016),
 - Year II (01/11/2016 – 31/10/2017),
 - Year III (01/11/2017 – 31/10/2018),
 - Year IV (01/11/2018 – 31/10/2019).



230 **Figure 2.** Annual and seasonal variations of the micrometeorological variables for the entire measurement period: (a) hourly means of air temperature (T_{air}), (b) daily means of relative humidity (RH), (c) hourly means of global radiation (R_g), (d) daily means of soil water content (SWC, left) and cumulative precipitation (P, right), (e) normalised difference vegetation index (NDVI) produced on 16-day intervals.



Mean annual temperature (T_{air}) during the study period (November 2015–October 2019) was 15.7°C for both sites (Fig. 2a, Table 1). Daily mean relative humidity ranged from a minimum of 6% in dry seasons up to 99 % during the growing seasons (Fig. 2b). Relative humidity (RH) was lowest in November and December, while the highest values were measured in February–May. Short wave incoming radiation (R_g) demonstrated typical seasonal fluctuations with higher values during the summer months (Fig. 2c, Table 1). The seasonal changes in R_g showed that the HG site had slightly higher values. The mean daily R_g during the four years measurement period were 240 and 250 W m^{-2} for the LG and HG sites, correspondingly. The peak values reached $1000\text{--}1200 \text{ W m}^{-2}$ in summer and $400\text{--}600 \text{ W m}^{-2}$ in winter.

240

Table 1. Summary of meteorological parameters: means of air temperature (T_{air}), soil water content (SWC), short-wave incoming radiation (R_g) and cumulative precipitation (P) in the growing seasons (January–May) and dry (June–December). Years I–IV defined as hydrological year (November–October).

		$T_{\text{air}} (^{\circ}\text{C})$		SWC (%)		P (mm)		$R_g (\text{W m}^{-2})$	
		LG	HG	LG	HG	LG	HG	LG	HG
Year I	growing season	16.7	16.9	0.151	0.101	318.5	316.1	237	249
	dry season	14.7	15	0.128	0.105	47.7	46.2	226	245
Year II	growing season	16.7	16.8	0.143	0.116	296.6	306.8	234	248
	dry season	14.2	14.9	0.122	0.104	68.3	67.4	268	255
Year III	growing season	16.1	15.9	0.176	0.117	401.9	377.8	248	251
	dry season	14.3	14	0.126	0.149	85.6	80.4	236	251
Year IV	growing season	16.1	14	0.138	0.119	286.3	257.7	238	242
	dry season	14.3	17	0.097	0.093	8.2	9.0	245	250

The LG and HG sites had mean annual precipitation of 378 mm and 365 mm, respectively. Approximately 55% of the total annual precipitation happened during the summer months (January–February), with autumn (March–May) as the second most humid season (approx. 30 %), winter (June–August) as the driest season with precipitation less than 10 mm per month and spring (September–November) characterized by short rain events (Fig. 2c, Table 1). Precipitation was highly variable during the measurement period. Years I and II were nearly the same as the long-term mean annual precipitation for the Karoo (376 mm and 365 mm in the LG site and 372 mm and 374 mm in the HG site) (du Toit et al., 2014). The last year of measurements was the driest year with annual precipitation rates of 295 and 267 mm for LG and HG sites, respectively, while Year III had the highest precipitation of 487 and 458 mm.

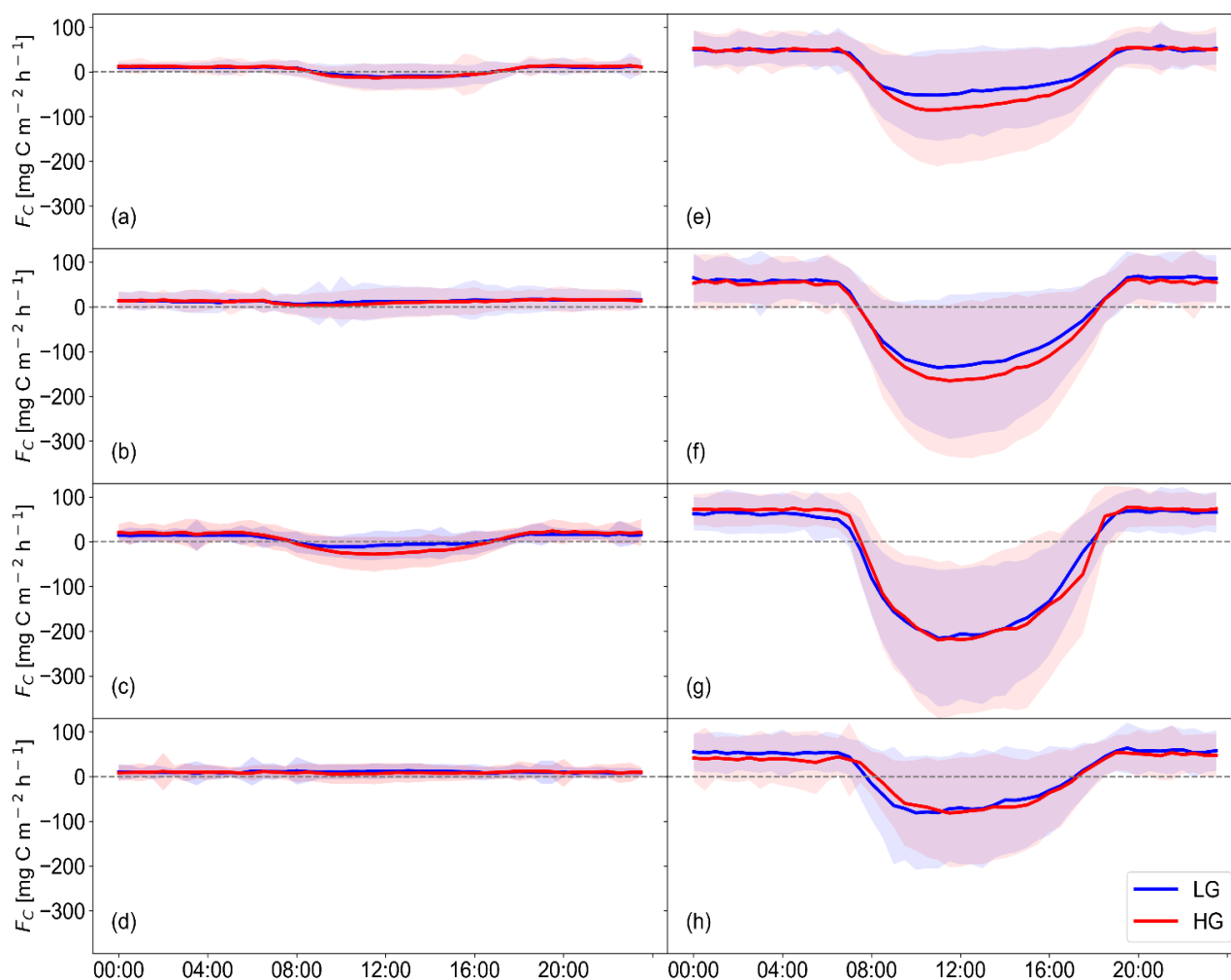
Seasonal variation of soil water content (SWC), expressed as volumetric water content, changed with the highest values in the summer and autumn months (growing season) and the lowest values during the winter (Fig. 2d, Table 1). The SWC values for the HG site were similar, however consistently slightly lower than those for the LG site. The highest values of SWC were in February–April 2018 (30 %) in the period with the highest precipitation, and the lowest in June–November 2019 (12 %), in the driest year over the measurement period.



The wind roses showed that the prevailing wind directions at the studied sites were NNW, N, NNE and SSE with the wind speed mainly between 1–6 m s⁻¹ (Fig. 1). The footprint indicates that around 90% of the carbon fluxes measured by the EC method were within the 70 m of the flux tower.

3.2 Diurnal patterns of carbon fluxes

The mean diurnal patterns of carbon fluxes are shown in Fig. 3 for each year and lumped together for the months of the dry (June–December) and growing (January–May) seasons.



265 **Figure 3.** Mean diurnal carbon fluxes in the dry (a–d) and growing (e–h) seasons for years I–VI (top to bottom) in the (blue) lenient grazing (LG) and (red) heavy grazing (HG) sites. Negative values indicate net carbon uptake, while positive values indicate net carbon release. Shading area indicates $\pm 1\sigma$.



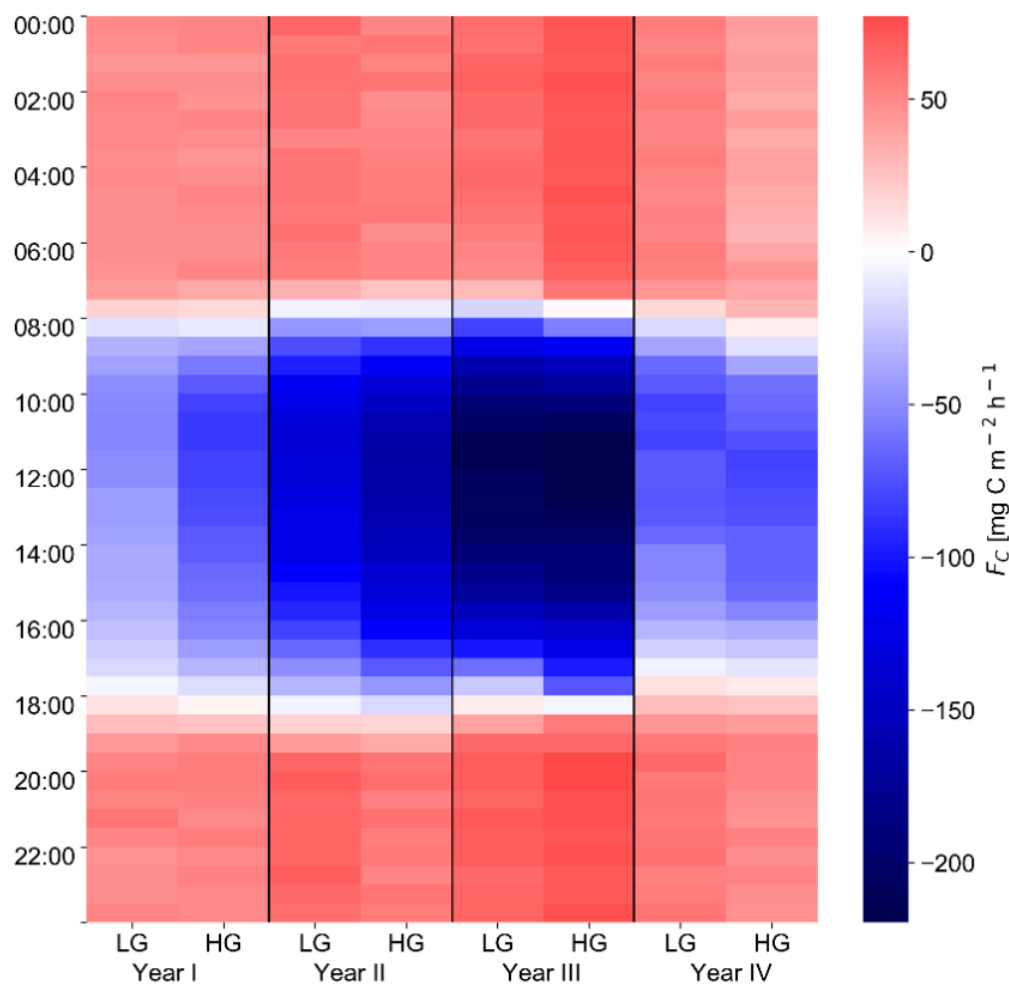
270 During the dry seasons (June–December), the ecosystems were inactive (Fig. 3a, b, c, d). The carbon fluxes values were close to zero for the most part as net carbon uptake was constrained due to water unavailability and vegetation dormancy. Mean diurnal carbon exchange rates in the dry seasons were the lowest in the year I and the highest in the year II (Table 2).

Table 2. Summary of mean diurnal carbon fluxes in $\text{mg C m}^{-2} \text{h}^{-1}$ of the dry (June–December) and growing (January–May) seasons for years I–IV. Years I–IV defined as hydrological year (November–October).

		F_C					
		min		mean		max	
		LG	HG	LG	HG	LG	HG
Year I	growing season	-51.83	-85.13	11.8	1.59	58.34	55.05
	dry season	-11.14	-13.31	4.0	4.13	12.94	14.03
Year II	growing season	-135.92	-165.43	-11.09	-25.01	68.62	62.33
	dry season	5.49	2.78	12.63	11.55	16.82	17.01
Year III	growing season	-215.69	-219.65	-33.80	-31.33	70.69	77.29
	dry season	-11.34	-27.89	6.2	4.19	17.85	24.23
Year IV	growing season	-81.18	-81.48	8.91	3.29	63.86	53.70
	dry season	7.35	5.97	10.13	9.05	13.01	12.59

275 During the growing seasons, the diurnal cycles of carbon fluxes for both sites demonstrate a classical behaviour with the carbon uptake predominating during the daytime and only respiration occurring during the night time (Fig. 3e, f, g, h). Mean diurnal carbon fluxes showed a net carbon uptake in the growing seasons of years II and III with average values of $-11.09 \text{ mg C m}^{-2} \text{h}^{-1}$ and $-25.01 \text{ mg C m}^{-2} \text{h}^{-1}$ (year II), $-33.80 \text{ mg C m}^{-2} \text{h}^{-1}$ and $-31.33 \text{ mg C m}^{-2} \text{h}^{-1}$ (year III) for the LG and HG sites, respectively. Maximum daytime mean carbon release and uptake were both observed in the year III (Table 2).

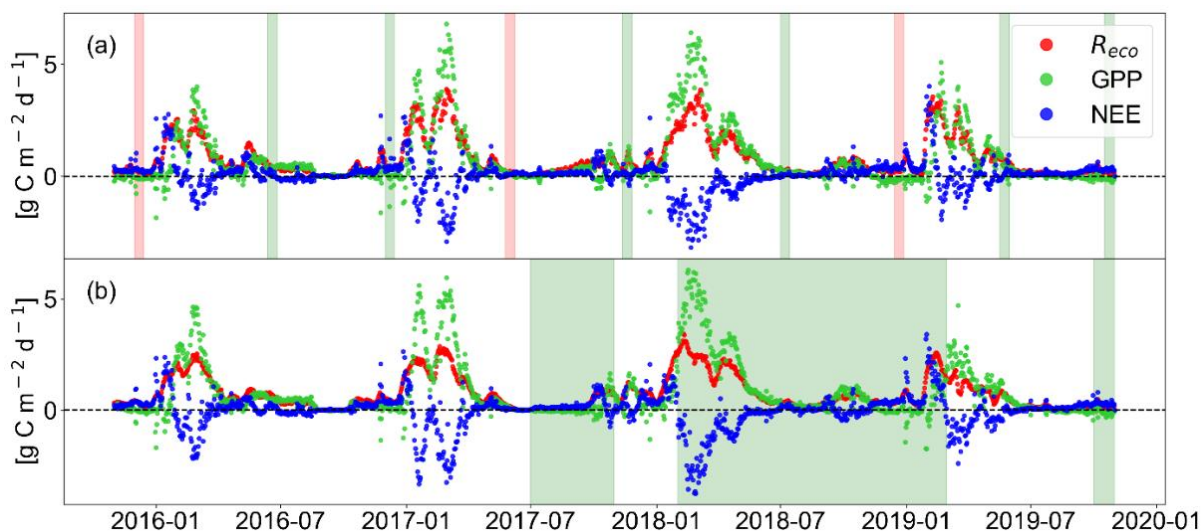
280 The ecosystems turned from a carbon source to a carbon sink mostly from 6:00 to 18:00 LT, with the highest carbon sequestration values near midday (Fig. 4). Midday uptake rates ranged from $48.15 \text{ mg C m}^{-2} \text{h}^{-1}$ (year I) to $206.04 \text{ mg C m}^{-2} \text{h}^{-1}$ (year III) for LG site and from $80.67 \text{ mg C m}^{-2} \text{h}^{-1}$ (year I) to $218.98 \text{ mg C m}^{-2} \text{h}^{-1}$ (year III) for the HG site.



285 **Figure 4.** Mean diurnal carbon fluxes fingerprint in the growing seasons (January–May) in the lenient grazing (LG) and heavy grazing (HG) sites. Blue colour represents net carbon uptake, while red indicates net carbon release.

3.3 Seasonal and annual NEE, GPP and R_{eco} variations

The NEE, R_{eco} and GPP at the studied sites varied seasonally with the peak values in the middle of the growing season (February–March) (Fig. 5, 6). Their seasonal patterns followed the changes in precipitation and SWC (Fig. 2d). The growing season lasted approximately 54 and 66 days (year I), 96 and 98 days (year II), 154 and 148 days (year III), and 95 and 96 days
290 (year IV) for the LG and HG sites, correspondingly (NEE < 0 on a daily basis). Throughout the measurement period, the studied ecosystems acted as a net carbon sink of 440 and 511 days (16 months) for the LG and HG sites, respectively.



295 **Figure 5.** Daily cumulative measured net ecosystem exchange (NEE) and partitioned component fluxes (i.e. gross primary production (GPP), ecosystem respiration (R_{eco})) across different grazing intensities for (a) lenient grazing (LG) and (b) heavy grazing (HG) sites. The green patterns represent recorded livestock period and the red patterns represent estimated livestock period.

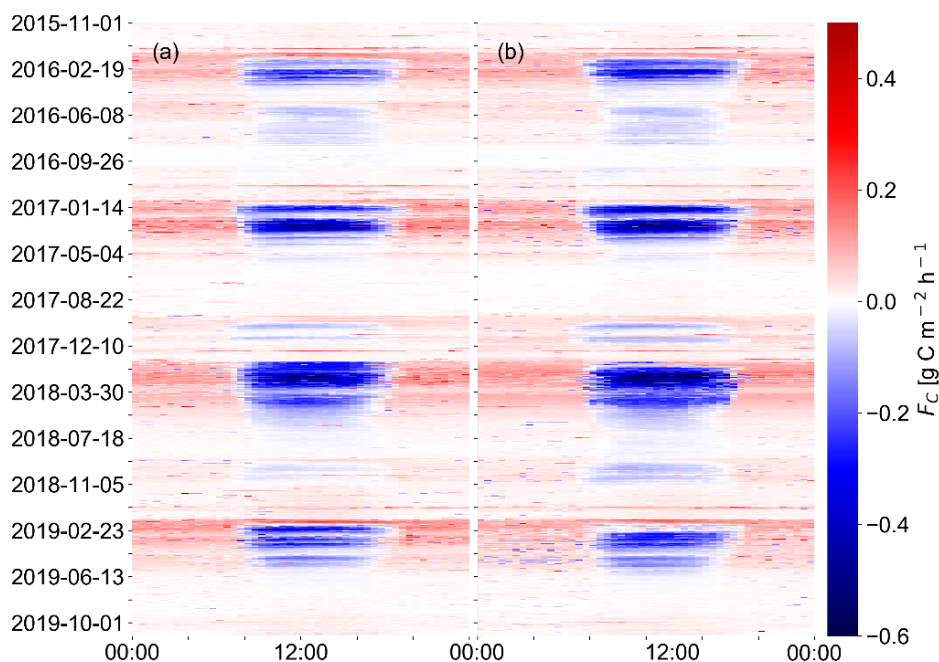


Figure 6. Temporal dynamics of the hourly carbon fluxes for the entire measurement period in the (a) lenient grazing (LG) and (b) heavy grazing (HG) sites.

The dry periods were mainly characterized by inactive ecosystems with low GPP, R_{eco} and NEE. Mean values of carbon fluxes throughout the measurement period for the growing and dry seasons were $-0.07 \text{ g C m}^{-2} \text{ d}^{-1}$ and $0.11 \text{ g C m}^{-2} \text{ d}^{-1}$ (LG), $-0.15 \text{ g C m}^{-2} \text{ d}^{-1}$ and $0.10 \text{ g C m}^{-2} \text{ d}^{-1}$ (HG).

300



Table 3. Daily cumulative net ecosystem exchange (NEE), ecosystem respiration (R_{eco}) and gross primary production (GPP) in $\text{g C m}^{-2} \text{d}^{-1}$. Years I–IV defined as hydrological year (November–October).

		NEE		R_{eco}	GPP
		min	max		
Year I	LG	−1.44	2.76	2.93	3.99
	HG	−2.17	2.39	2.54	4.64
Year II	LG	−2.91	2.69	3.88	6.79
	HG	−3.31	2.64	2.88	5.96
Year III	LG	−3.18	2.60	3.85	6.40
	HG	−3.74	2.06	3.44	6.31
Year IV	LG	−1.93	4.02	3.54	5.09
	HG	−2.39	3.41	2.58	4.71

305

At the LG site, the magnitude of the daily NEE during the measurement period varied from $-3.18 \text{ g C m}^{-2} \text{d}^{-1}$ to $4.02 \text{ g C m}^{-2} \text{d}^{-1}$. At the HG site, it ranged from $-3.74 \text{ g C m}^{-2} \text{d}^{-1}$ to $3.41 \text{ g C m}^{-2} \text{d}^{-1}$ (Table 3).

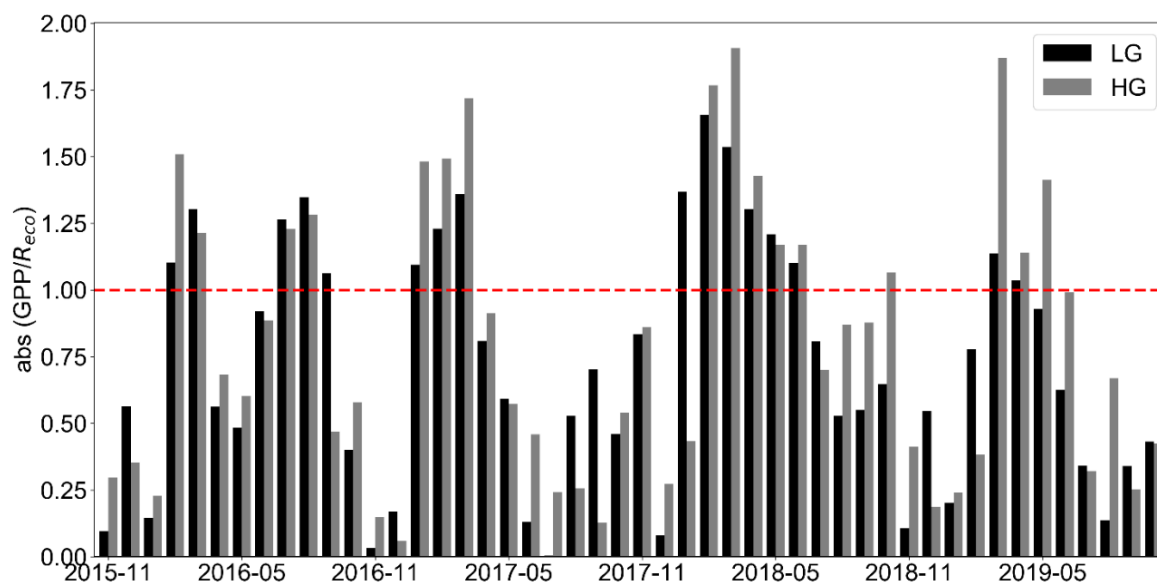


Figure 7. Absolute monthly ratios of gross primary production (GPP) versus ecosystem respiration (R_{eco}) in the (black) lenient grazing (LG) and (grey) heavy grazing (HG) sites. $GPP/R_{eco} > 1$ ratios revealing a net carbon uptake.

310

At both sites, R_{eco} was always highest during the growing season and decreased in the dry season with the lowest R_{eco} in June–October. The highest daily sums of R_{eco} were in the year III, whereas the lowest daily sums were in the year I for both sites (Table 3). Similarly, the GPP was highest during the growing season. During the dry seasons, the maximum GPP ranged from $0.39 \text{ g C m}^{-2} \text{d}^{-1}$ to $1.43 \text{ g C m}^{-2} \text{d}^{-1}$ for the LG site and from $0.58 \text{ g C m}^{-2} \text{d}^{-1}$ to $1.65 \text{ g C m}^{-2} \text{d}^{-1}$ for the HG site. Both R_{eco}



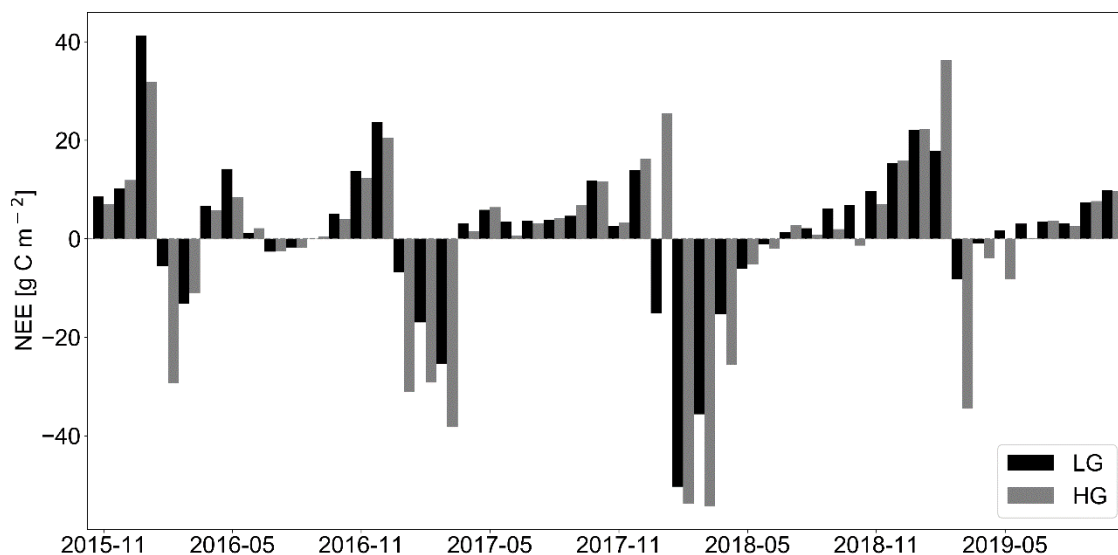
315 and GPP were higher at the LG site as compared to the HG site (Fig.5 a, b) with the absolute values of the GPP/R_{eco} ratios revealing a net carbon uptake ($GPP/R_{eco} > 1$) during most of the growing season (Fig. 7).

3.4 Carbon balance

Carbon budgets were estimated on the monthly, seasonal and annual scales to demonstrate the carbon source/sink strength of the studied sites. During the dry seasons, the LG site released on average $6.05 \text{ g C m}^{-2} \text{ month}^{-1}$, while the HG site released
 320 $5.30 \text{ g C m}^{-2} \text{ month}^{-1}$ (Fig. 8, Table 4). The highest carbon release for both sites was measured in December 2016 (year II). Dry season carbon sequestration on a monthly basis was observed only during July–August 2016 (cumulative precipitation 35 mm) (Table 4). Although only slight differences were found between the years I–IV in the dry seasons, significant fluctuations were observed during the growing seasons. The carbon sequestration periods varied throughout the measurement period in length (2 to 6 months) and in the strength of carbon sequestration. The monthly cumulative NEE showed the highest carbon
 325 sequestration rates in February 2018 for the LG site and in March 2018 for the HG site, and the highest carbon release in January 2016 for the LG site and in February 2019 for the HG site (Table 4).

Table 4. Monthly cumulative net ecosystem exchange (NEE) in g C m^{-2} . Years I–IV defined as hydrological year (November–October).

		Nov	Dec	Jan	Feb	Mar	Apr	May	Jun	Jul	Aug	Sep	Oct
Year I	LG	8.54 ± 4.51	10.23 ± 4.49	41.18 ± 4.35	-5.66 ± 5.45	-13.18 ± 5.10	6.62 ± 4.64	14.17 ± 7.64	1.16 ± 10.29	-2.64 ± 6.52	-1.79 ± 6.98	-0.04 ± 9.81	5.09 ± 6.95
	HG	6.93 ± 6.13	11.92 ± 4.53	31.84 ± 5.38	-29.33 ± 5.94	-10.99 ± 5.26	5.82 ± 4.62	8.47 ± 7.67	2.15 ± 11.44	-2.53 ± 6.57	-1.83 ± 6.26	0.51 ± 6.26	4.05 ± 5.77
Year II	LG	13.79 ± 4.25	23.68 ± 4.18	-6.82 ± 4.96	-17.01 ± 4.80	-25.37 ± 6.51	3.16 ± 5.08	5.86 ± 4.87	3.40 ± 6.55	3.70 ± 6.29	3.88 ± 5.56	4.61 ± 4.54	11.82 ± 4.26
	HG	12.35 ± 4.24	20.50 ± 4.03	-31.12 ± 5.66	-29.23 ± 6.31	-38.27 ± 7.01	1.56 ± 5.75	6.41 ± 4.92	0.69 ± 6.34	3.18 ± 6.66	4.19 ± 5.08	6.76 ± 4.97	11.64 ± 4.81
Year III	LG	2.52 ± 5.42	13.94 ± 4.24	-15.08 ± 13.52	-50.37 ± 6.00	-35.66 ± 6.35	-15.31 ± 7.50	-6.08 ± 7.93	-1.10 ± 5.53	1.37 ± 4.66	2.11 ± 5.41	6.18 ± 4.21	6.87 ± 4.20
	HG	3.24 ± 6.40	16.26 ± 6.93	25.46 ± 6.47	-53.79 ± 20.75	-54.27 ± 21.67	-25.64 ± 21.42	-5.28 ± 10.99	-2.04 ± 6.46	2.73 ± 5.88	0.81 ± 5.33	1.93 ± 4.51	-1.42 ± 4.30
Year IV	LG	9.69 ± 4.84	15.38 ± 4.99	22.07 ± 4.77	17.75 ± 6.66	-8.23 ± 7.37	-1.01 ± 5.51	1.72 ± 5.89	3.03 ± 4.60	3.51 ± 3.82	3.19 ± 5.96	7.35 ± 4.84	9.88 ± 5.22
	HG	7.01 ± 5.73	15.80 ± 4.10	22.32 ± 3.83	36.30 ± 9.30	-34.57 ± 11.94	-3.93 ± 5.71	-8.20 ± 5.96	0.06 ± 4.22	3.67 ± 3.24	2.64 ± 5.33	7.63 ± 4.52	9.65 ± 4.53



330 **Figure 8.** Monthly cumulative net ecosystem exchange (NEE) for the entire measurement period in the (black) lenient grazing (LG) and
 (grey) heavy grazing (HG) sites.

The seasonal NEE for the dry season of year I showed the lowest carbon release rates (Table 5). Similar NEE was observed
 during the dry season of year III. Meanwhile, dry season of year II demonstrated the highest carbon release with year IV
 demonstrating only slightly lower rates of carbon release (Table 5). During the growing seasons of years I and IV, carbon
 335 release was observed on a seasonal basis. In comparison, years II and III showed enhanced carbon sequestration with the
 highest carbon uptake in the year III for both sites.

Table 5. Seasonal net ecosystem exchange (NEE) and precipitation (P) in the growing (January–May) and dry (June–December) seasons.
 Years I–IV defined as hydrological year (November–October).

		NEE (g C m ⁻²)		P (mm)	
		LG	HG	LG	HG
Year I	growing season	43.13 ±20.65	5.81 ±21.45	318.5	316.1
	dry season	20.54 ±37.76	21.22 ±34.75	47.7	46.2
Year II	growing season	-40.17 ±18.85	-90.65 ±21.63	296.6	306.8
	dry season	64.87 ±28.24	59.32 ±28.89	68.3	67.4
Year III	growing season	-122.51 ±30.04	-113.54 ±43.34	401.9	377.8
	dry season	31.89 ±25.98	21.51 ±28.89	85.6	80.4
Year IV	growing season	32.31 ±21.26	13.42 ±25.45	286.3	257.7
	dry season	52.03 ±25.99	46.47 ±30.89	8.2	9

340

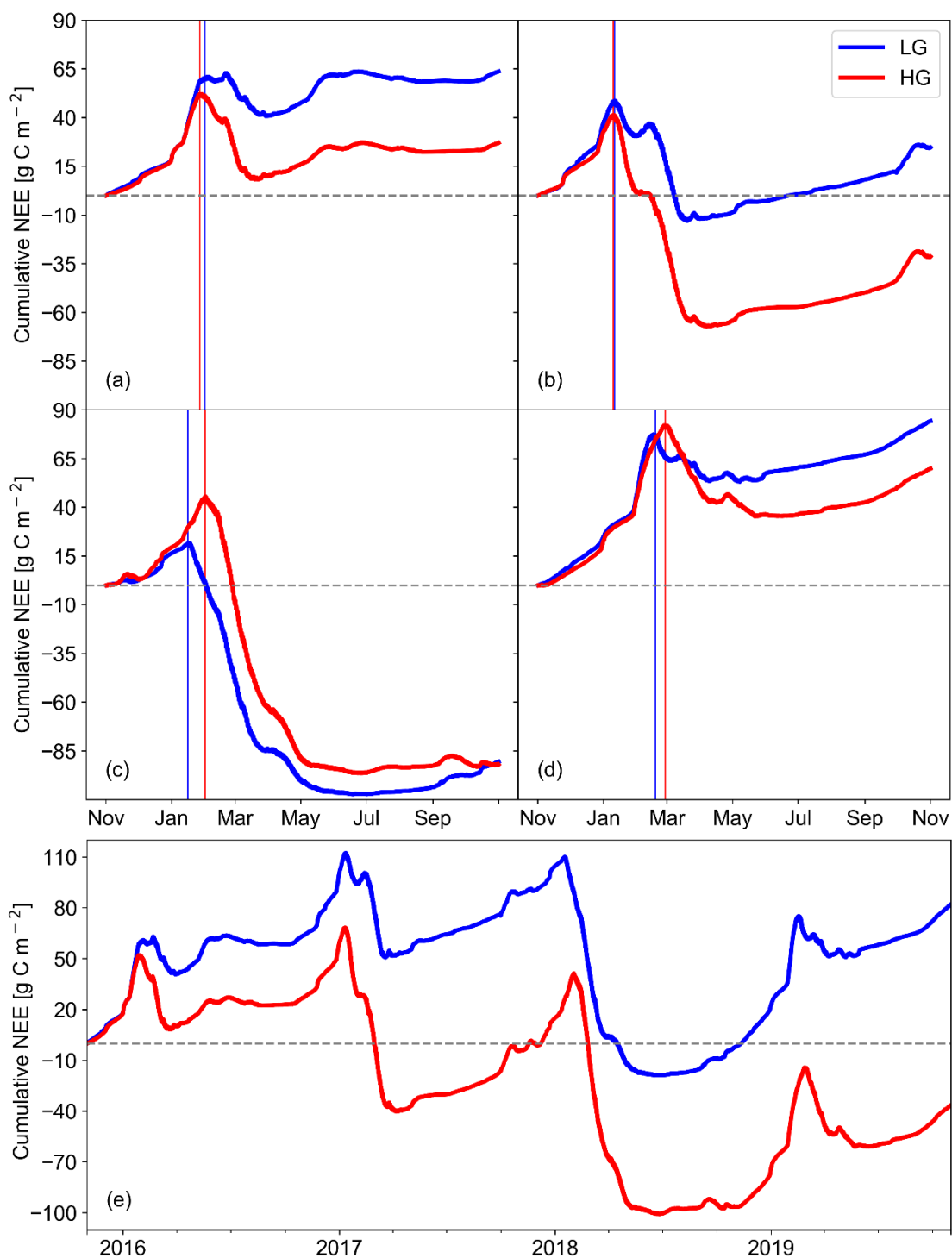


Figure 9. Annual cumulative net ecosystem exchange (NEE) (a–d) for the years I–IV with vertical lines indicating the highest respiration point throughout the year when ecosystem turning into a carbon sink and (e) four years cumulative NEE in the (blue) lenient grazing (LG) and (red) heavy grazing (HG) sites.



345 Annually integrated cumulative NEE varied from carbon sink to source over the four years measurement period (Fig. 9). Only year III of the four years had negative NEE (i.e. were net carbon sinks at the annual timescale) for the LG site and years II–III for the HG site. In the year I, the total cumulative NEE was higher for the LG site ($63.68 \pm 55.59 \text{ g C m}^{-2} \text{ yr}^{-1}$) compared to the HG site ($27.03 \pm 53.24 \text{ g C m}^{-2} \text{ yr}^{-1}$). In the year II, however, a sequestration of $31.33 \pm 47.44 \text{ g C m}^{-2} \text{ yr}^{-1}$ was measured for the HG site compared to a release of $24.69 \pm 44.27 \text{ g C m}^{-2} \text{ yr}^{-1}$ at the LG site. In the year III, both sites acted as carbon
 350 sinks with sequestration rates of $90.61 \pm 51.39 \text{ g C m}^{-2} \text{ yr}^{-1}$ (LG) and $92.02 \pm 66.73 \text{ g C m}^{-2} \text{ yr}^{-1}$ (HG). In year IV, impacted by drought, carbon uptake was limited by water availability even during the peak of the wet season in summer. It resulted in carbon release rates of $84.33 \pm 43.76 \text{ g C m}^{-2} \text{ yr}^{-1}$ (LG) and $59.89 \pm 46.11 \text{ g C m}^{-2} \text{ yr}^{-1}$ (HG). After the four years measurement period, the total cumulative NEE indicated a carbon release of $82.11 \pm 48.75 \text{ g C m}^{-2}$ for the LG site while the HG site was a slight carbon sink with a sequestration rate of $36.43 \pm 53.38 \text{ g C m}^{-2}$.

355 3.5 Correlation between NDVI and GPP

We investigated the relationship between each NDVI (each 16 days) and the corresponding daily sums of GPP (Fig. 10). High leaf area leads to a higher light absorption capacity, and hence result in a higher GPP when water availability is sufficient. The NDVI values range from zero (no vegetation) to 1 (dense vegetation).

360 **Table 6.** Statistical summary of normalised difference vegetation index (NDVI) in the growing (January–May) and dry (June–December) seasons. Years I–IV defined as hydrological year (November–October).

		NDVI					
		LG			HG		
		min	mean	max	min	mean	max
Year I	growing season	0.20	0.31	0.41	0.21	0.33	0.52
	dry season	0.19	0.23	0.30	0.19	0.25	0.29
Year II	growing season	0.25	0.38	0.63	0.24	0.40	0.72
	dry season	0.19	0.21	0.25	0.19	0.21	0.24
Year III	growing season	0.19	0.43	0.61	0.19	0.44	0.68
	dry season	0.19	0.23	0.29	0.19	0.22	0.26
Year IV	growing season	0.19	0.35	0.48	0.20	0.36	0.53
	dry season	0.19	0.21	0.24	0.19	0.21	0.23

Overall mean NDVI in the dry seasons was 0.22 for both sites (Fig. 2e, Table 6) with the lowest NDVI values during spring (September–November). The mean values in the growing seasons were 0.37 and 0.38 for the LG and HG sites, respectively.
 365 The maximum NDVI values were measured in mid-February in the years II and III (Table 6). Mean annual NDVI values were

0.27 and 0.28 in the year I, and 0.29 and 0.30 in the year II for LG and HG sites, respectively. In the years III and IV, the mean NDVI values were 0.32 and 0.27 for both sites.

Analysis of the seasonal trends of NDVI and derived GPP demonstrated strong linear correlations (p -value < 0.0001) between them for both studied sites (Fig. 10). The coefficient of determination ranged from 0.65 to 0.93 for the LG site and from 0.71 to 0.96 for the HG site.

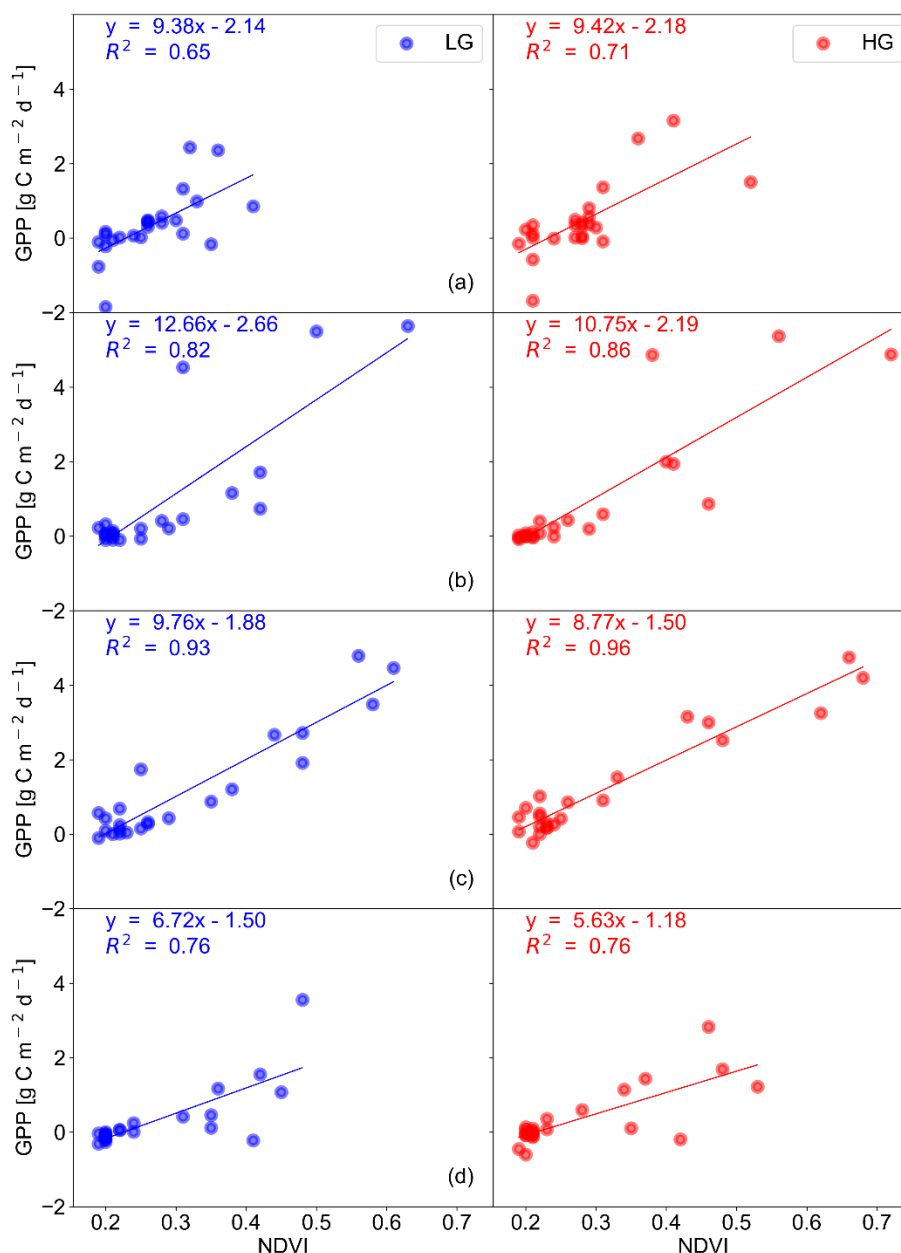


Figure 10. Correlation between normalised difference vegetation index (NDVI) and gross primary production (GPP) for the years I–IV (a–d) in the (blue) lenient grazing (LG) and (red) heavy grazing (HG) sites.



4 Discussion

375 This study provides new understanding of the impact of current and past grazing intensities on CO₂ fluxes and their daily, seasonal, and annual dynamics in semi-arid South African ecosystems. We found that the two investigated grazing regimes under similar climate, soil conditions and topography have highly influenced plant species composition and vegetation cover leading to implications for their role as potential grazing areas and/or efficient CO₂ sinks in the future.

4.1 Effect of livestock grazing on carbon sink strength

380 4.1.1 Impacts of overgrazing via altered vegetation cover

After four years of measurements, our results indicate that the HG ecosystem was unexpectedly a slight carbon sink, while the LG ecosystem was a considerable carbon source, thereby disproving our hypothesis of the LG site being a stronger sink for atmospheric CO₂. The differences in carbon fluxes between the studied sites could be explained by different vegetation cover (species distribution as well as aboveground biomass) due to overgrazing in the past. During the resting period, the HG site showed consistently slightly higher mean NDVI and had slightly higher NDVI peaks compared to the LG site. Increases in canopy cover after a long resting period were reported by several authors (Chen et al., 2014; Lin et al., 2011; Mofidi et al., 2013). Yan et al. (2014) reported that long-term heavy livestock grazing resulted in significant decrease of soil C and N storage, which may significantly alter the ecosystem causing decrease in the carbon sequestration rates. The HG system is dominated by unpalatable grasses, while nearly all palatable shrubs have been extirpated by overgrazing. Zhou et al. (2012) showed that the fine root biomass of perennial grasses was more abundant in the upper soil layer compared to shrubs. It implies that grasses are stronger competitors for water, especially in water-limited ecosystems with pulsed precipitation. This coincides with our finding that in the spring (September–November), the studied sites were net sources of carbon for all measurement years, with the exception of the HG site during October 2018 with 15 mm of precipitation (Table 4, Fig. 8). The difference was likely due to the vegetation cover at the HG site, being dominated by grasses, and thus able to respond more quickly to rain events due to shallow-root systems that use discontinuous and erratic water sources in the upper soil layers compared with the shrubs deep-root systems that use water in deeper soil layers (Canadell et al., 1996; Hipondoka et al., 2003; Zhou et al., 2012). *Aristida diffusa* is a drought tolerant dominant grass at the HG site that managed to survive the intense summer drought, although net mortality of other grass species was observed (du Toit and O'Connor, 2020). Furthermore, Zhou et al. (2012) found that total soil organic carbon storage was higher for perennial grasses (higher soil organic carbon inputs through primary production and slower return of carbon through decomposition) than for shrubs.

The differences in carbon budgets between the studied sites indicate that a long resting period (2007–2017) along with transition to unpalatable drought resistant grass species at the previously overgrazed site improved the carbon sink potential (HG site had higher carbon sequestration rates compared to the LG site) due to an increase in the canopy cover. At the same time, the site is unfavourable from the perspective of the current livestock grazing system, and restoring its original species composition would return its value as pasture. Leu et al. (2014) showed that heavily grazed shrubland (northern Negev, Israel)



can be recovered within <16 years by implementing strict conservation management. Seymour et al. (2010) reported that 20 years of recovery period in the Karoo degraded ecosystems restored grazing potential, while not returning all palatable species.

4.1.2 Impacts of lenient temporary vs. continuous heavy livestock grazing

At the HG site, a slight decrease in the carbon uptake peaks was linked to an increase of continuous grazing time (Figs. 3, 5).
410 Figure 3 shows that during the resting period (I and II years), the HG site had a significantly higher mean diurnal NEE compared to the LG site with rotational grazing. However, during the years III and IV, the mean diurnal NEE patterns were similar for both sites. This could be explained by continuous livestock grazing, which began in July 2017 at the HG site. The impacts of livestock grazing on the ecosystems were associated in previous studies with canopy cover, the response of the dominant plant species to grazing, different grazing regimes, and site history (Chen et al., 2014; Gan et al., 2012; K'Otuto et
415 al., 2013; Kairis et al., 2015; Lecain et al., 2000; Räsänen et al., 2017; Tagesson et al., 2015; Talore et al., 2016; Wagle et al., 2019; Yan et al., 2017). In a study conducted in Chinese and Mongolian steppes, Na et al. (2018) showed that continuous grazing leads to reduction in aboveground biomass (AGB). Ma et al. (2019) found a strong correlation between grazing intensity and vegetation indexes (AGB and NDVI). At high grazing intensity, canopy cover and vegetation indexes showed a decreasing trend (Amiri et al., 2008; Belgacem et al., 2013; Ping et al., 2018; Sun et al., 2011) resulting in a higher percentage
420 of the soil surface exposed to radiation, followed by increased evaporation and decrease in SWC (Chen et al., 2013; Villegas et al., 2014; Yan et al., 2016, 2017). In our study, analysis of the NDVI trends supported the interpretation of the impacts of continuous grazing: mean NDVI values decreased in the HG site due to persistent livestock grazing and resulted in the same mean values for both sites in the years III and IV (Sect. 3.5, Fig. 2e).

Our results showed a strong positive correlation between the NDVI and the daily sums of GPP for both studied sites (Fig. 10).
425 Previous studies also reported a strong linear correlation between the GPP and NDVI in the grassland, shrubland and savanna ecosystems (Huang et al., 2019; Yan et al., 2019). The seasonal GPP peaks followed the course of the NDVI variations. The HG site had slightly higher coefficients of determination in the Years I–III than the LG site. The natural state of the HG site was disturbed by heavy livestock grazing followed by a change in species composition to unpalatable grass species, which made the site robust concerning the drought conditions. In the Year IV, both sites had similar correlations. It shows that the
430 long continuous grazing at the HG site has a negative impact on the vegetation cover, which also affects carbon exchange.

4.2 Water availability as the main driver of inter-annual variability of carbon fluxes

While we could attribute differences in CO₂ exchange between sites to grazing intensity, sums and their variability on an annual basis were still highly dominated by the amount of available water, as reported in previous studies conducted in similar systems (Merbold et al., 2009 and references therein). During the growing seasons, carbon fluxes were negative in the daytime
435 (correlated with light intensity throughout the day) and positive at nighttime (changed to carbon release after the sunset). At the beginning of the growing season, during the onset of summer precipitation events, an immediate response of R_{eco} to precipitation and plant germination was observed. First precipitation event also caused an increase in GPP to some extent, but



the NEE was comparatively small during the plant germination phase due to high respiration. However, during the peak of the growing season, GPP exceeded R_{eco} and the ecosystems turned into a carbon sink. This is consistent with other findings in the semi-arid ecosystems (Kutsch et al., 2008; Merbold et al., 2009; Tagesson et al., 2015, 2016; Williams and Albertson, 2005). During the dry seasons, the ecosystems were not physiologically active due to the limited water availability. These findings are in line with other studies conducted in African ecosystems (Archibald et al., 2009; Brümmer et al., 2008; Räsänen et al., 2017; Tagesson et al., 2015; Veenendaal et al., 2004). Mean carbon fluxes showed the highest carbon uptake and release rates in the year III, followed by the year II. It is in line with the temporal distribution of precipitation and NDVI indexes. Based on NDVI data, year II stands for the highest NDVI peak, whereas year III represents the wettest year with the longest NDVI peaks (the longest growing season), years I and IV represent the lowest NDVI peaks due to the distribution (year I) and the deficit of precipitation (year IV).

At the annual scale, the carbon sink strength in the studied sites varied annually depending on the climatic conditions. Years I and II had similar precipitation rates (373 mm and 370 mm) (Fig. 2d, Table 1). The LG site acted as a carbon source in both periods but in the year II with lower strength compared to the year I, whereas the HG site was a carbon source in the year I and carbon sink in the year II (Fig. 9). The differences in the carbon sequestration rates between years I and II were determined by different precipitation distribution which resulted into the short growing season in the year I. During the transition period (November–December) sites received only 10 mm of precipitation in the year I compared to the year II (47 mm). During the peak of the growing seasons (January–March), both sites received 230 mm and 280 mm of precipitation for the years I and II, respectively. At the end of the growing season (April–May), both sites had higher amount of precipitation in the year I (88 mm) than in the year II (23 mm). During the dry months (June–October) of year I, both sites received 47 mm of precipitation, which explains carbon sink months in the dry period (July–August), while during the dry season of the year II, sites received only 20 mm. Fig.2d shows that the same amount falls within two rainy periods in the year II causing a longer and delayed soil moisture decay leading to a longer growing season than in year I, where more equally distributed rain led to a faster dry up. In the year III, both sites acted as considerable carbon sinks (Fig. 9) due to the increased precipitation and, as a result, increased length of the growing season (Table 1). In the year IV, the studied ecosystems acted as considerable carbon sources with the highest CO_2 release due to the precipitation deficit compared to the long-term mean annual precipitation (approximately 25 %). Our results agree with other, previously mentioned studies, which observed similar seasonal dynamics of NEE in their respective regions (Brümmer et al., 2008; Jongen et al., 2011; Quansah et al., 2015; Tagesson et al., 2015, 2016; Veenendaal et al., 2004; Xu and Baldocchi, 2004).

Similar annual NEE of $-98 \text{ g C m}^{-2} \text{ yr}^{-1}$ to $21 \text{ g C m}^{-2} \text{ yr}^{-1}$ were observed by Scott et al. (2010) in the Kendall grassland, USA with mean annual precipitation of 345 mm (63 % in the summer months). Räsänen et al. (2016) observed annual carbon budgets of $-85 \text{ g C m}^{-2} \text{ yr}^{-1}$, $67 \text{ g C m}^{-2} \text{ yr}^{-1}$ and $139 \text{ g C m}^{-2} \text{ yr}^{-1}$ (2011–2013) in the Welgegund atmospheric measurement station grassland ecosystem, South Africa (540 mm). The annual NEE ranges at the South African Kruger National Park were from $-138 \text{ g C m}^{-2} \text{ yr}^{-1}$ to $155 \text{ g C m}^{-2} \text{ yr}^{-1}$ with a mean annual precipitation of 550 mm (Archibald et al., 2009). Niu et al. (2020)



reported a carbon source ecosystem with carbon release ranging from $34.99 \text{ C m}^{-2} \text{ yr}^{-1}$ to $63.05 \text{ g C m}^{-2} \text{ yr}^{-1}$ in a semi-arid sandy grassland ecosystem in northern China (360 mm).

On a broader context, Valentini et al. (2014) reported a small carbon sink of $0.61 \pm 0.58 \text{ Pg C yr}^{-1}$ ($-20.1 \text{ g C m}^{-2} \text{ yr}^{-1}$) on a whole continent on an annual basis by averaging out all the estimates. This can be compared with measured here mean annual
475 NEE of $20.57 \text{ g C m}^{-2} \text{ yr}^{-1}$ for LG site and $-9.11 \text{ g C m}^{-2} \text{ yr}^{-1}$ for HG site. However, complete and accurate estimation of the carbon budget for the African continent is not available due to large gaps in carbon fluxes data from in situ measurements for many African ecosystems. Thus, understanding the dynamics of carbon fluxes in different types of ecosystems is crucial to underpin these larger-scale estimations.

5 Conclusions

480 We analysed four years of measured CO_2 fluxes from 1 November 2015 to 31 October 2019 at two semi-arid Karoo (South Africa) ecosystems with different grazing intensities. To our knowledge, the current study provides the first long-term EC measurement of carbon fluxes, which are compared between semi-arid ecosystems with similar climatic conditions but different past and present grazing intensity in South Africa. Unexpectedly, the site with continuous heavy grazing after a long resting period was more efficient as a CO_2 sink. This was linked to a higher abundance of unpalatable grasses, which may be
485 better able to compete for water. At the same time, the high ratio of unpalatable vs palatable species made this site less suitable for its current use as sheep pasture. This may signify that an optimally managed grazing site is not necessarily the most carbon efficient ecosystem. Slight decreases in the carbon uptake peaks were observed in response to resuming heavy grazing at the HG site (years III–IV) by modification of the SWC, soil properties and aboveground biomass.

The interannual variability of carbon budgets was mainly driven by the annual amount and seasonal distribution of
490 precipitation. The annual cumulative NEE varied from $-92.02 \text{ g C m}^{-2} \text{ yr}^{-1}$ (year III at the HG site) to $84.33 \text{ g C m}^{-2} \text{ yr}^{-1}$ (year IV at the LG site) demonstrating that semi-arid Karoo ecosystems under livestock grazing can act as a carbon source or carbon sink, depending on meteorological (precipitation) conditions. Our study contributes to a better understanding of livestock grazing effects on the ecosystem–atmosphere carbon exchange in the semi-arid Karoo ecosystems. It may have important implications on the design of sustainable grazing strategies in the region.

495 Appendix A. Latent and sensible heat fluxes and energy balance closure

Half-hourly time-series of the latent and sensible heat fluxes are shown in Figure A1. During February–April (growing season) turbulent energy fluxes were dominated by latent heat flux, while during May–January they were dominated by sensible heat flux. During the growing season, the night-time peaks for the latent and sensible heat fluxes were 90 W m^{-2} and 45 W m^{-2} , while daytime peaks reached 400 W m^{-2} and 470 W m^{-2} (Table A1). Peak latent and sensible heat flux values in the dry seasons
500 were 55 W m^{-2} and 75 W m^{-2} during night-time, and reached the maximum of 250 W m^{-2} and 500 W m^{-2} during daytime. The



four-year means of H, LE, G and Rn were 65 W m^{-2} , 24 W m^{-2} , 15 W m^{-2} , 213 W m^{-2} for the LG site and 71 W m^{-2} , 24 W m^{-2} , 14 W m^{-2} , 250 W m^{-2} for the HG site. Also, Rn was slightly higher in the dry seasons than in the growing seasons.

505 **Table A1. Summary of energy balance components: means of sensible heat (H), latent heat (LE), ground heat flux (G), net radiation (Rn) in the growing (Jan–May) and dry (Jun–Dec) seasons. Years I–IV defined as hydrological year (Nov–Oct).**

		H (W m^{-2})		LE (W m^{-2})		G (W m^{-2})		Rn (W m^{-2})	
		LG	HG	LG	HG	LG	HG	LG	HG
Year I	growing season	48	49	37	38	-0.37	1.67	105	116
	dry season	59	62	8	9	3.87	6.89	99	113
Year II	growing season	44	51	39	37	0.20	-5.51	110	126
	dry season	60	66	11	11	9.47	4.15	132	142
Year III	growing season	47	55	41	42	0.93	1.41	119	152
	dry season	59	61	12	16	4.28	3.73	95	113
Year IV	growing season	52	52	31	32	0.90	1.21	105	117
	dry season	66	68	7	8	4.32	6.17	87	95

The partitioning of the turbulent energy can be additionally analysed by examining the H/Rn and LE/Rn ratios. During the peak of the growing seasons, the H/Rn ratios were 0.22 and 0.27, whereas during the dry periods, those ratios were 0.70 and 0.68 for the LG and HG sites, respectively. The LE/Rn ratios during the growing and dry periods were 0.73 and 0.18 for the
 510 LG site, and 0.65 and 0.18 for the HG site.

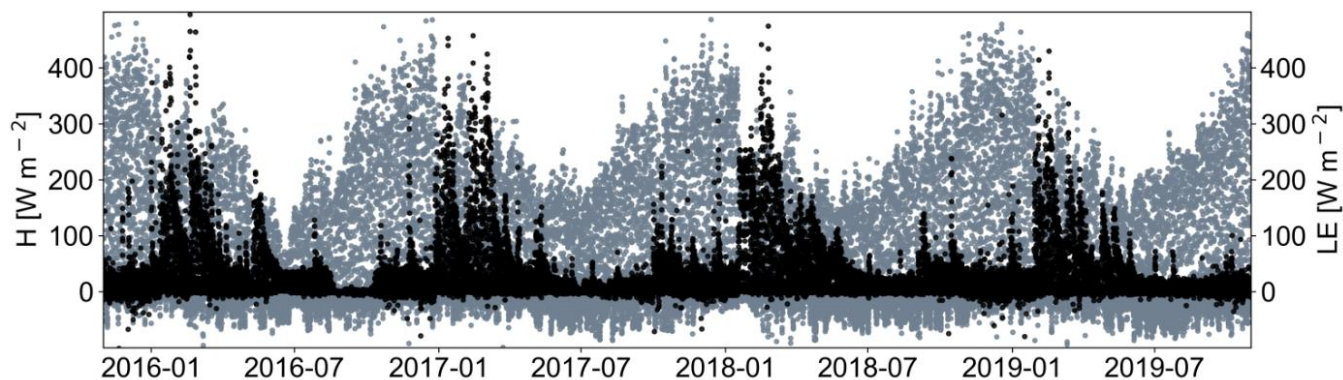
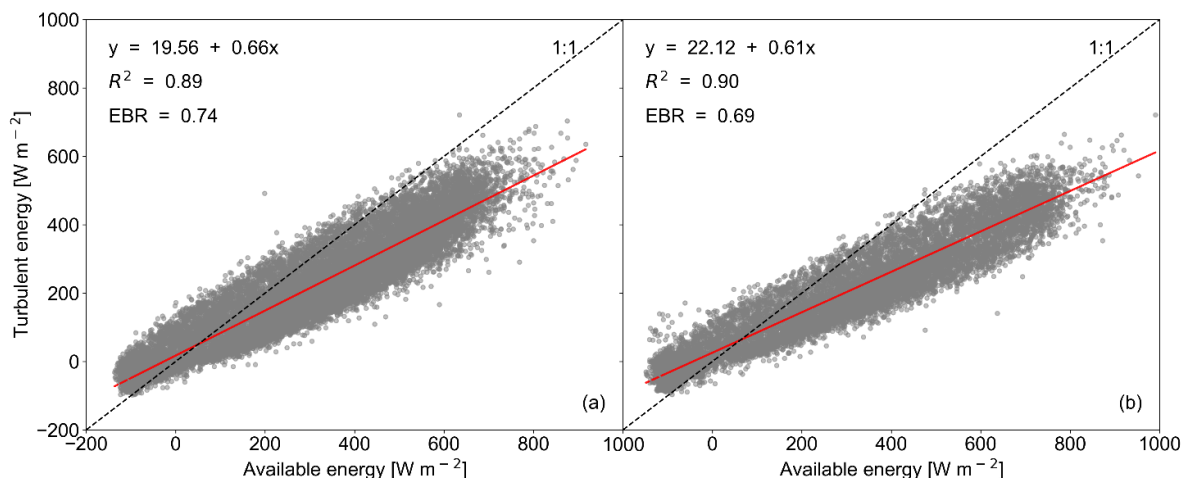


Figure A1. Half-hourly time-series of the sensible heat (H, grey dots) and latent heat (LE, black dots) fluxes.



515 **Figure A2.** Energy balance closure (EBC) determined by turbulent energy fluxes ($H + LE + SH + SLE$) versus available energy ($R_n - G - S_g$): in the (a) lenient grazing (LG) and (b) heavy grazing (HG) sites.

The half-hourly data of G , R_n , H and LE were used to evaluate and analyse EBC for the entire study period based on the linear regression statistics between the turbulent and available energy (Fig. A2). The numbers of half-hourly data used for EBC evaluation were 19,698 and 13,955 for LG and HG sites, correspondingly. No seasonal trends were found. The regression fits
 520 between turbulent energy and available energy reveal a strong linear relation with coefficients of determination (R^2) of 0.89 and 0.90 for the LG and HG sites. The intercepts and slopes were 19.56 and 0.66 for the LG site, and 22.12 and 0.61 for the HG site, respectively. The EBRs for the entire study period were 0.74 for the LG site and 0.69 for the HG site. The residual of the surface energy balance during daytime ranged from -154 W m^{-2} to 479 W m^{-2} and from -169 W m^{-2} to 513 W m^{-2} with highest values between 10:00 and 12:00 for the LG and HG sites, respectively (Fig. A3). During the night-time the residual
 525 varied from -132 W m^{-2} to 56 W m^{-2} and from -134 W m^{-2} to 91 W m^{-2} for the LG and HG sites.

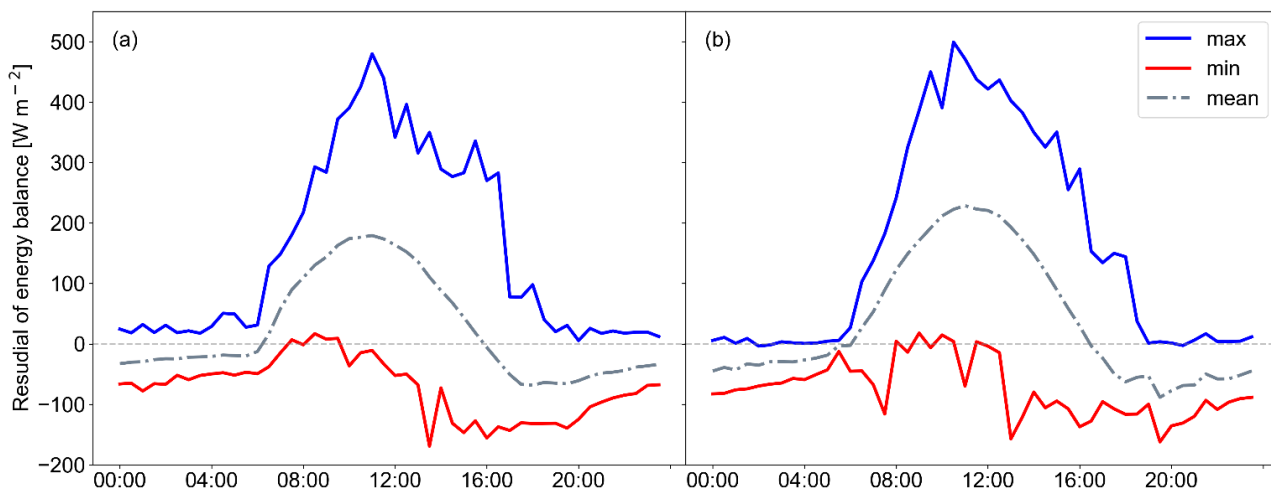




Figure A3. Maximum (blue), mean (grey) and minimum (red) diurnal variation of the residual of the energy balance in the (a) lenient grazing (LG) and (b) heavy grazing (HG) sites.

530 *Data availability.* Data used in this study can be requested from Oksana Rybchak (oksana.rybchak@thuenen.de). Furthermore, the data will be uploaded to the Fluxnet database.

535 *Author contributions.* CB, GF and OR conceived the study. JP, KM, JKJ, JdT installed and managed the eddy covariance flux towers, collected the raw data. JdT provided information about the studied sites (biodiversity, grazing management) and helped to write a corresponding sub-section in the methodology part. CT provided the remote sensing-based vegetation MODIS indices and wrote a corresponding sub-section in the methodology part. CB, GF, MB gave scientific advice to the overall data analysis and interpretation. OR wrote the manuscript, processed raw data, conducted flux data analysis and interpretation. All authors discussed and reviewed the manuscript.

Competing interests. The authors declare that they have no conflict of interest.

540 *Acknowledgements.* The authors acknowledge funding from the German Federal Ministry of Education and Research (BMBF), framework programmes SPACES and SPACES II (Science Partnerships for the Assessment of Complex Earth System Processes in Southern Africa), projects ARS AfricaE (grant number 01LL1303A) and EMSAfrica (grant number 01LL1801E).

References

- Ago, E. E., Agbossou, E. K., Cohard, J. M., Galle, S. and Aubinet, M.: Response of CO₂ fluxes and productivity to water availability in two contrasting ecosystems in northern Benin (West Africa), *Ann. For. Sci.*, 73(2), 483–500, doi:10.1007/s13595-016-0542-9, 2016.
- 545 Ahlström, A., Raupach, M. R., Schurgers, G., Smith, B., Arneth, A., Jung, M., Reichstein, M., Canadell, J. G., Friedlingstein, P., Jain, A. K., Kato, E., Poulter, B., Sitch, S., Stocker, B. D., Viovy, N., Wang, Y. P., Wiltshire, A., Zaehle, S. and Zeng, N.: The dominant role of semi-arid ecosystems in the trend and variability of the land CO₂ sink, *Science* (80-.), 348(6237), 895–899, doi:10.1126/science.aaa1668, 2015.
- 550 Amiri, F., Ariapour, A. and Fadai, S.: Effects of livestock grazing on vegetation composition and soil moisture properties in grazed and non-grazed range site, *J. Biol. Sci.*, 8(8), 1289–1297, doi:10.3923/jbs.2008.1289.1297, 2008.
- Anthoni, P. M., Knohl, A., Rebmann, C., Freibauer, A., Mund, M., Ziegler, W., Kolle, O. and Schulze, E. D.: Forest and agricultural land-use-dependent CO₂ exchange in Thuringia, Germany, *Glob. Chang. Biol.*, 10(12), 2005–2019, doi:10.1111/j.1365-2486.2004.00863.x, 2004.
- Araújo, A. C., Nobre, A. D., Kruijt, B., Elbers, J. A., Dallarosa, R., Stefani, P., Von Randow, C., Manzi, A. O., Culf, A. D., 555 Gash, J. H. C., Valentini, R. and Kabat, P.: Comparative measurements of carbon dioxide fluxes from two nearby towers in a central Amazonian rainforest: The Manaus LBA site, *J. Geophys. Res.*, 107(D20), 1–20, doi:10.1029/2001jd000676, 2002.
- Archibald, S. A., Kirton, A., Van Der Merwe, M. R., Scholes, R. J., Williams, C. A. and Hanan, N.: Drivers of inter-annual



- variability in Net Ecosystem Exchange in a semi-arid savanna ecosystem, South Africa, *Biogeosciences*, 6(2), 251–266, doi:10.5194/bg-6-251-2009, 2009.
- 560 Ardö, J., Mölder, M., El-Tahir, B. A. and Elkhidir, H. A. M.: Seasonal variation of carbon fluxes in a sparse savanna in semi arid Sudan, *Carbon Balance Manag.*, 3, 1–18, doi:10.1186/1750-0680-3-7, 2008.
- Aubinet, M., Grelle, A., Ibrom, A., Rannik, Ü., Moncrieff, J., Foken, T., Kowalski, A. S., Martin, P. H., Berbigier, P., Bernhofer, C., Clement, R., Elbers, J., Granier, A., Grünwald, T., Morgenstern, K., Pilegaard, K., Rebmann, C., Snijders, W., Valentini, R. and Vesala, T.: Estimates of the Annual Net Carbon and Water Exchange of Forests: The EUROFLUX
565 Methodology, *Adv. Ecol. Res.*, 30(C), 113–175, doi:10.1016/S0065-2504(08)60018-5, 2000.
- Aubinet, M., Feigenwinter, C., Heinesch, B., Laffineur, Q., Papale, D., Reichstein, M., Rinne, J. and Gorsel, E. Van: Nighttime Flux Correction, in *Eddy Covariance: A Practical Guide to Measurement and Data Analysis*, Springer Atmospheric Sciences., 2012.
- Baldocchi, D., Olson, R. and Hollinger, D. Y.: ScholarWorks at University of Montana Numerical Terradynamic Simulation
570 Group FLUXNET : A New Tool to Study the Temporal and Spatial Variability of Ecosystem-Scale Carbon Dioxide , Water Vapor , and Energy Flux Densities Let us know how access to this doc, *Bull. Am. Meteorol. Soc.*, 0477(May 2014), 2415–2434, doi:10.1175/1520-0477(2001)082<2415, 2001.
- Baldocchi, D. D.: Assessing the eddy covariance technique for evaluating carbon dioxide exchange rates of ecosystems: Past, present and future, *Glob. Chang. Biol.*, 9(4), 479–492, doi:10.1046/j.1365-2486.2003.00629.x, 2003.
- 575 Baldocchi, D. D., Hicks, B. B. and Meyers, T. P.: Measuring biosphere-atmosphere exchanges of biologically related gases with micrometeorological methods, *Ecology*, 69(5), 1331–1340, doi:10.2307/1941631, 1988.
- Bao, K., Tian, H., Su, M., Qiu, L., Wei, X., Zhang, Y., Liu, J., Gao, H. and Cheng, J.: Stability of ecosystem CO₂ flux in response to changes in precipitation in a semiarid grassland, *Sustain.*, 11(9), 1–18, doi:10.3390/su11092597, 2019.
- Belgacem, A. O., Al Kaabi, N., Al Wawi, H. and Louhaichi, M.: Effect of livestock grazing on plant cover and species diversity
580 in desert rangelands: A case study of Musawar Al Ottoria in Qatar, *Range Manag. Agrofor.*, 34(1), 88–92, 2013.
- Béziat, P., Ceschia, E. and Dedieu, G.: Carbon balance of a three crop succession over two cropland sites in South West France, *Agric. For. Meteorol.*, 149(10), 1628–1645, doi:10.1016/j.agrformet.2009.05.004, 2009.
- Brand, T. S.: Grazing behaviour and diet selection by Dorper sheep, *Small Rumin. Res.*, 36(2), 147–158, doi:10.1016/S0921-4488(99)00158-3, 2000.
- 585 Brümmer, C., Falk, U., Papen, H., Szarzynski, J., Wassmann, R. and Brüggemann, N.: Diurnal, seasonal, and interannual variation in carbon dioxide and energy exchange in shrub savanna in Burkina Faso (West Africa), *J. Geophys. Res. Biogeosciences*, 113(2), 1–11, doi:10.1029/2007JG000583, 2008.



- Burba, G.: Eddy Covariance Method-for Scientific, Industrial, Agricultural, and Regulatory Applications, LI-COR Biosciences, Lincoln, Nebraska Copyright., 2013.
- 590 Canadell, J., Jackson, R. B., Ehleringer, J. R., Mooney, H. A., Sala, O. E. and Schulze, E.-D.: Max rooting depth of veg types at global scale, *Oecologia*, 108, 538–595, 1996.
- Cao, M., Zhang, Q. and Shugart, H. H.: Dynamic responses of African ecosystem carbon cycling to climate change, *Clim. Res.*, 17(2 SPECIAL 8), 183–193, doi:10.3354/cr017183, 2001.
- Chen, D., Zheng, S., Shan, Y., Taube, F. and Bai, Y.: Vertebrate herbivore-induced changes in plants and soils: Linkages to ecosystem functioning in a semi-arid steppe, *Funct. Ecol.*, 27(1), 273–281, doi:10.1111/1365-2435.12027, 2013.
- 595 Chen, J., Shi, W. and Cao, J.: Effects of Grazing on Ecosystem CO₂ Exchange in a Meadow Grassland on the Tibetan Plateau During the Growing Season, *Environ. Manage.*, 55(2), 347–359, doi:10.1007/s00267-014-0390-z, 2014.
- Chimner, R. A. and Welker, J. M.: Influence of grazing and precipitation on ecosystem carbon cycling in a mixed-grass prairie, *Pastoralism*, 1(1), 1–15, doi:10.1186/2041-7136-1-20, 2011.
- 600 Delgado-Balbuena, J., Arredondo, J. T., Loeschner, H. W., Pineda-Martínez, L. F., Carbajal, J. N. and Vargas, R.: Seasonal Precipitation Legacy Effects Determine the Carbon Balance of a Semiarid Grassland, *J. Geophys. Res. Biogeosciences*, 124(4), 987–1000, doi:10.1029/2018JG004799, 2019.
- Department of Agriculture Fisheries and Forestry: South Africa – Biomes, OpenAfrica [online] Available from: <https://africaopendata.org/dataset/e2ef64dd-6577-4a73-9eff-87f677b2dd92/resource/620721d9-2605-44dc-81f8-efb5af9169da/download/rsabiome4xkhi.zip%0A%0A>, 2013.
- 605 Didan, K., Munoz, A. B., Solano, R. and Huete, A.: MODIS Vegetation Index User 's Guide (Collection 6), The University of Arizona., 2015.
- Falge, E. M., Clement, R. J., Baldocchi, D. D., Dolman, H., Burba, G. G., Anthoni, P., Aubinet, M., Olson, R., Bernhofer, C., Ceulemans, R. and Granier, A.: Gap filling strategies for defensible annual sums of net ecosystem exchange, *Agric. For. Meteorol.*, 107, 43–69, 2001.
- 610 Fei, X., Jin, Y., Zhang, Y., Sha, L., Liu, Y., Song, Q., Zhou, W., Liang, N., Yu, G., Zhang, L., Zhou, R., Li, J., Zhang, S. and Li, P.: Eddy covariance and biometric measurements show that a savanna ecosystem in Southwest China is a carbon sink, *Sci. Rep.*, 7(February), 1–14, doi:10.1038/srep41025, 2017.
- Finkelstein, P. L. and Sims, P. F.: Sampling error in eddy correlation flux measurements, *J. Geophys. Res.*, 106(D4), 3503–3509, doi:10.1029/2000JD900731, 2001.
- 615 Foken, T. and Wichura, B.: Tools for quality assessment of surface-based flux measurements, *Agric. For. Meteorol.*, 78(1–2), 83–105, doi:10.1016/0168-1923(95)02248-1, 1996.



- Foken, T., Göckede, M., Mauder, M., Mahrt, L., Amiro, B. and Munger, W.: Post-Field Data Quality Control, in Handbook of Micrometeorology, edited by X. Lee, W. Massman, and B. Law, pp. 181–208, Springer., 2006.
- 620 Frank, A. B.: Carbon dioxide fluxes over a grazed prairie and seeded pasture in the Northern Great Plains, *Environ. Pollut.*, 116(3), 397–403, doi:10.1016/S0269-7491(01)00216-0, 2002.
- Gan, L., Peng, X., Peth, S. and Horn, R.: Effects of grazing intensity on soil thermal properties and heat flux under *Leymus chinensis* and *Stipa grandis* vegetation in Inner Mongolia, China, *Soil Tillage Res.*, 118, 147–158, doi:10.1016/j.still.2011.11.005, 2012.
- 625 Gash, J. H. C. and Culf, A. D.: Applying a linear detrend to eddy correlation data in realtime, *Boundary-Layer Meteorol.*, 79(3), 301–306, doi:10.1007/bf00119443, 1996.
- Goulden, M. L., Munger, J. W., Fan, S. M., Daube, B. C. and Wofsy, S. C.: Measurements of carbon sequestration by long-term eddy covariance: Methods and a critical evaluation of accuracy, *Glob. Chang. Biol.*, 2(3), 169–182, doi:10.1111/j.1365-2486.1996.tb00070.x, 1996.
- 630 Gourlez de la Motte, L., Mamadou, O., Beckers, Y., Bodson, B., Heinesch, B. and Aubinet, M.: Rotational and continuous grazing does not affect the total net ecosystem exchange of a pasture grazed by cattle but modifies CO₂ exchange dynamics, *Agric. Ecosyst. Environ.*, 253(November 2017), 157–165, doi:10.1016/j.agee.2017.11.011, 2018.
- Groendahl, L., Friberg, T. and Soegaard, H.: Temperature and snow-melt controls on interannual variability in carbon exchange in the high Arctic, *Theor. Appl. Climatol.*, 88(1–2), 111–125, doi:10.1007/s00704-005-0228-y, 2007.
- 635 Gu, L., Falge, E. M., Boden, T., Baldocchi, D. D., Black, T. A., Saleska, S. R., Suni, T., Verma, S. B., Vesala, T., Wofsy, S. C. and Xu, L.: Objective threshold determination for nighttime eddy flux filtering, *Agric. For. Meteorol.*, 128(3–4), 179–197, doi:10.1016/j.agrformet.2004.11.006, 2005.
- Hansis, E., Davis, S. J. and Pongratz, J.: Relevance of methodological choices for accounting of land use change carbon fluxes, *Global Biogeochem. Cycles*, 29(8), 1230–1246, doi:10.1002/2014GB004997, 2015.
- 640 Hipondoka, M. H. T., Aranibar, J. N., Chirara, C., Lihavha, M. and Macko, S. A.: Vertical distribution of grass and tree roots in arid ecosystems of Southern Africa: Niche differentiation or competition?, *J. Arid Environ.*, 54(2), 319–325, doi:10.1006/jare.2002.1093, 2003.
- Huang, X., Xiao, J. and Ma, M.: Evaluating the performance of satellite-derived vegetation indices for estimating gross primary productivity using FLUXNET observations across the globe, *Remote Sens.*, 11(15), doi:10.3390/rs11151823, 2019.
- 645 Huete, A. R., Justice, C., van Leeuwen, W., Jacobson, A., Solanos, R. and Laing, T. D.: MODIS VEGETATION INDEX (MOD 13) ALGORITHM THEORETICAL BASIS DOCUMENT Version 3, Arizona., 1999.
- Hulme, M., Doherty, R., Ngara, T., New, M. and Lister, D.: African climate change: 1900-2100, *Clim. Res.*, 17(2 SPECIAL



- 8), 145–168, doi:10.3354/cr017145, 2001.
- Huxman, T. E., Snyder, K. A., Tissue, D., Leffler, A. J., Ogle, K., Pockman, W. T., Sandquist, D. R., Potts, D. L. and
650 Schwinning, S.: Precipitation pulses and carbon fluxes in semiarid and arid ecosystems, *Oecologia*, 141(2), 254–268,
doi:10.1007/s00442-004-1682-4, 2004.
- Ivans, S., Hipps, L., Leffler, A. J. and Ivans, C. Y.: Response of water vapor and CO₂ fluxes in semiarid lands to seasonal and
intermittent precipitation pulses, *J. Hydrometeorol.*, 7(5), 995–1010, doi:10.1175/JHM545.1, 2006.
- Jongen, M., Pereira, J. S., Aires, L. M. I. and Pio, C. A.: The effects of drought and timing of precipitation on the inter-annual
655 variation in ecosystem-atmosphere exchange in a Mediterranean grassland, *Agric. For. Meteorol.*, 151(5), 595–606,
doi:10.1016/j.agrformet.2011.01.008, 2011.
- Jung, M., Reichstein, M., Schwalm, C. R., Huntingford, C., Sitch, S., Ahlström, A., Arneth, A., Camps-Valls, G., Ciais, P.,
Friedlingstein, P., Gans, F., Ichii, K., Jain, A. K., Kato, E., Papale, D., Poulter, B., Raduly, B., Rödenbeck, C., Tramontana,
G., Viovy, N., Wang, Y. P., Weber, U., Zaehle, S. and Zeng, N.: Compensatory water effects link yearly global land CO₂ sink
660 changes to temperature, *Nature*, 541(7638), 516–520, doi:10.1038/nature20780, 2017.
- K’Otuto, G. O., Otieno, D. O., Seo, B., Ogindo, H. O. and Onyango, J. C.: Carbon dioxide exchange and biomass productivity
of the herbaceous layer of a managed tropical humid savanna ecosystem in western Kenya, *J. Plant Ecol.*, 6(4), 286–297,
doi:10.1093/jpe/rts038, 2013.
- Kairis, O., Karavitis, C., Salvati, L., Kounalaki, A. and Kosmas, K.: Exploring the Impact of Overgrazing on Soil Erosion and
665 Land Degradation in a Dry Mediterranean Agro-Forest Landscape (Crete, Greece), *Arid L. Res. Manag.*, 29(3), 360–374,
doi:10.1080/15324982.2014.968691, 2015.
- Kutsch, W. L., Hanan, N., Scholes, R. J., McHugh, I., Kubheka, W., Eckhardt, H. and Williams, C.: Response of carbon fluxes
to water relations in a savanna ecosystem in South Africa, *Biogeosciences Discuss.*, 5(3), 2197–2235, doi:10.5194/bg-d-5-
2197-2008, 2008.
- 670 Lasslop, G., Reichstein, M., Papale, D., Richardson, A., Arneth, A., Barr, A., Stoy, P. and Wohlfahrt, G.: Separation of net
ecosystem exchange into assimilation and respiration using a light response curve approach: Critical issues and global
evaluation, *Glob. Chang. Biol.*, 16(1), 187–208, doi:10.1111/j.1365-2486.2009.02041.x, 2010.
- Lecain, D. R., Morgan, J. A., Schuman, G. E., Reeder, J. D. and Hart, R. H.: Carbon exchange rates in grazed and ungrazed
pastures of Wyoming, *J. Range Manag.*, 53(2), 199–206, doi:10.2307/4003283, 2000.
- 675 Leu, S., Mussery, A. M. and Budovsky, A.: The effects of long time conservation of heavily grazed shrubland: A case study
in the Northern Negev, Israel, *Environ. Manage.*, 54(2), 309–319, doi:10.1007/s00267-014-0286-y, 2014.
- Lin, X., Zhang, Z., Wang, S., Hu, Y., Xu, G., Luo, C., Chang, X., Duan, J., Lin, Q., Xu, B., Wang, Y., Zhao, X. and Xie, Z.:



- Response of ecosystem respiration to warming and grazing during the growing seasons in the alpine meadow on the Tibetan plateau, *Agric. For. Meteorol.*, 151(7), 792–802, doi:10.1016/j.agrformet.2011.01.009, 2011.
- 680 van Lingen, M.: [Afrikaner/ Hereford compositional data 2018]. Unpublished data, 2018.
- Lucas-Moffat, A. M., Huth, V., Augustin, J., Brümmer, C., Herbst, M. and Kutsch, W. L.: Towards pairing plot and field scale measurements in managed ecosystems: Using eddy covariance to cross-validate CO₂ fluxes modeled from manual chamber campaigns, *Agric. For. Meteorol.*, 256–257(August 2016), 362–378, doi:10.1016/j.agrformet.2018.01.023, 2018.
- Massman, W. J. and Lee, X.: Massman_2002_Eddy covariance flux correlations and uncertainties in long-term studies of
685 carbon and energy exchanges.pdf, *Agric. For. Meteorol.*, 113, 121–144, doi:10.1016/S0168-1923(02)00105-3, 2002.
- Mauder, M. and Foken, T.: Documentation and Instruction Manual of the Eddy-Covariance Software Package TK3, *Arbeitsergebnisse*, 3(46), 60, ISSN 1614-8916, doi:10.5281/zenodo.20349, 2011.
- Mauder, M., Cuntz, M., Drüe, C., Graf, A., Rebmann, C., Schmid, H. P., Schmidt, M. and Steinbrecher, R.: A strategy for quality and uncertainty assessment of long-term eddy-covariance measurements, *Agric. For. Meteorol.*, 169, 122–135,
690 doi:10.1016/j.agrformet.2012.09.006, 2013.
- Merbold, L., Ardö, J., Arneeth, A., Scholes, R. J., Nouvellon, Y., De Grandcourt, A., Archibald, S., Bonnefond, J. M., Boulain, N., Brueggemann, N., Bruemmer, C., Cappelaere, B., Ceschia, E., El-Khidir, H. A. M., El-Tahir, B. A., Falk, U., Lloyd, J., Kergoat, L., Le Dantec, V., Mougou, E., Muchinda, M., Mukelabai, M. M., Ramier, D., Roupsard, O., Timouk, F., Veenendaal, E. M. and Kutsch, W. L.: Precipitation as driver of carbon fluxes in 11 African ecosystems, *Biogeosciences*, 6(6), 1027–1041,
695 doi:10.5194/bg-6-1027-2009, 2009.
- Meza, F. J., Montes, C., Bravo-Martínez, F., Serrano-Ortiz, P. and Kowalski, A. S.: Soil water content effects on net ecosystem CO₂ exchange and actual evapotranspiration in a Mediterranean semiarid savanna of Central Chile, *Sci. Rep.*, 8(1), 1–11, doi:10.1038/s41598-018-26934-z, 2018.
- Miranda, J. D., Armas, C., Padilla, F. M. and Pugnaire, F. I.: Climatic change and rainfall patterns: Effects on semi-arid plant
700 communities of the Iberian Southeast, *J. Arid Environ.*, 75(12), 1302–1309, doi:10.1016/j.jaridenv.2011.04.022, 2011.
- Moffat, A. M., Papale, D., Reichstein, M., Hollinger, D. Y., Richardson, A. D., Barr, A. G., Beckstein, C., Braswell, B. H., Churkina, G., Desai, A. R., Falge, E., Gove, J. H., Heimann, M., Hui, D., Jarvis, A. J., Kattge, J., Noormets, A. and Stauch, V. J.: Comprehensive comparison of gap-filling techniques for eddy covariance net carbon fluxes, *Agric. For. Meteorol.*, 147(3–4), 209–232, doi:10.1016/j.agrformet.2007.08.011, 2007.
- 705 Mofidi, M., Jafari, M., Tavili, A., Rashtbari, M. and Alijanpour, A.: Grazing Exclusion Effect on Soil and Vegetation Properties in Imam Kandi Rangelands, Iran, *Arid L. Res. Manag.*, 27(1), 32–40, doi:10.1080/15324982.2012.719575, 2013.
- Moncrieff, J., Clement, R., Finnigan, J. and Meyers, T.: Averaging, Detrending, and Filtering of Eddy Covariance Time Series,



- in Handbook of Micrometeorology, pp. 7–31., 2006.
- 710 Moncrieff, J. B., Massheder, J. M., De Bruin, H., Elbers, J., Friborg, T., Heusinkveld, B., Kabat, P., Scott, S., Soegaard, H. and Verhoef, A.: A system to measure surface fluxes of momentum, sensible heat, water vapour and carbon dioxide, *J. Hydrol.*, 188–189(1–4), 589–611, doi:10.1016/S0022-1694(96)03194-0, 1997.
- Mucina, L., Rutherford, M. C., Palmer, A. R., Milton, S. J., Scott, L., Lloyd, J. W., der Merwe, B., Hoare, D. B., Bezuidenhout, H., Vlok, J. H. J., Euston-Brown, D. I. W., Powrie, L. W. and Dold, A. P.: Nama-Karoo Biome, in *The vegetation of South Africa, Lesotho and Swaziland*, edited by L. Mucina and M. C. Rutherford, pp. 324–347, SANBI, Pretoria., 2006.
- 715 Müller, C., Eickhout, B., Zaehle, S., Bondeau, A., Cramer, W. and Lucht, W.: Effects of changes in CO₂, climate, and land use on the carbon balance of the land biosphere during the 21st century, *J. Geophys. Res. Biogeosciences*, 112(2), G02032, doi:10.1029/2006JG000388, 2007.
- Na, Y., Li, J., Hoshino, B., Bao, S., Qin, F. and Myagmarseren, P.: Effects of different grazing systems on aboveground biomass and plant species dominance in typical Chinese and Mongolian steppes, *Sustain.*, 10(12), doi:10.3390/su10124753, 720 2018.
- Nagy, M. T., Janssens, I. A., Curiel Yuste, J., Carrara, A. and Ceulemans, R.: Footprint-adjusted net ecosystem CO₂ exchange and carbon balance components of a temperate forest, *Agric. For. Meteorol.*, 139(3–4), 344–360, doi:10.1016/j.agrformet.2006.08.012, 2006.
- 725 Nakano, T. and Shinoda, M.: Interannual variation in net ecosystem CO₂ exchange and its climatic controls in a semiarid grassland of mongolia, *J. Agric. Meteorol.*, 74(2), 92–96, doi:10.2480/agrmet.D-17-00035, 2018.
- Niu, Y., Li, Y., Yun, H., Wang, X., Gong, X., Duan, Y. and Liu, J.: Variations in diurnal and seasonal net ecosystem carbon dioxide exchange in a semiarid sandy grassland ecosystem in China ’ s Horqin, *Biogeosciences*, Preprint(April), 1–40, doi:<https://doi.org/10.5194/bg-2020-89>, 2020.
- 730 Otieno, D. O., K’Otuto, G. O., Maina, J. N., Kuzyakov, Y. and Onyango, J. C.: Responses of ecosystem carbon dioxide fluxes to soil moisture fluctuations in a moist Kenyan savanna, *J. Trop. Ecol.*, 26(6), 605–618, doi:10.1017/S0266467410000416, 2010.
- Papale, D., Reichstein, M., Aubinet, M., Canfora, E., Bernhofer, C., Kutsch, W., Longdoz, B., Rambal, S., Valentini, R., Vesala, T. and Yakir, D.: Towards a standardized processing of Net Ecosystem Exchange measured with eddy covariance technique: Algorithms and uncertainty estimation, *Biogeosciences*, 3(4), 571–583, doi:10.5194/bg-3-571-2006, 2006.
- 735 Pastorello, G., Trotta, C., Canfora, E., Chu, H., Christianson, D., Cheah, Y. W., Poindexter, C., Chen, J., Elbashandy, A., Humphrey, M., Isaac, P., Polidori, D., Ribeca, A., van Ingen, C., Zhang, L., Amiro, B., Ammann, C., Arain, M. A., Ardö, J., Arkebauer, T., Arndt, S. K., Arriga, N., Aubinet, M., Aurela, M., Baldocchi, D., Barr, A., Beamesderfer, E., Marchesini, L.



- B., Bergeron, O., Beringer, J., Bernhofer, C., Berveiller, D., Billesbach, D., Black, T. A., Blanken, P. D., Bohrer, G., Boike, J., Bolstad, P. V., Bonal, D., Bonnefond, J. M., Bowling, D. R., Bracho, R., Brodeur, J., Brümmer, C., Buchmann, N., Burban, 740 B., Burns, S. P., Buysse, P., Cale, P., Cavagna, M., Cellier, P., Chen, S., Chini, I., Christensen, T. R., Cleverly, J., Collalti, A., Consalvo, C., Cook, B. D., Cook, D., Coursolle, C., Cremonese, E., Curtis, P. S., D'Andrea, E., da Rocha, H., Dai, X., Davis, K. J., De Cinti, B., de Grandcourt, A., De Ligne, A., De Oliveira, R. C., Delpierre, N., Desai, A. R., Di Bella, C. M., di Tommasi, P., Dolman, H., Domingo, F., Dong, G., Dore, S., Duce, P., Dufrière, E., Dunn, A., Dušek, J., Eamus, D., Eichelmann, U., ElKhidir, H. A. M., Eugster, W., Ewenz, C. M., Ewers, B., Famulari, D., Fares, S., Feigenwinter, I., Feitz, A., 745 Fensholt, R., Filippa, G., Fischer, M., Frank, J., Galvagno, M., Gharun, M., Gianelle, D., et al.: The FLUXNET2015 dataset and the ONEFlux processing pipeline for eddy covariance data, *Sci. data*, 7(1), 225, doi:10.1038/s41597-020-0534-3, 2020.
- Ping, Y., Qiang, Z., Yang, Y., Zhang, L., Zhang, H., Hao, X. and Sun, X.: Seasonal and inter-annual variability of the Bowen smith ratio over a semi-arid grassland in the Chinese Loess Plateau, *Agric. For. Meteorol.*, 252(April 2017), 99–108, doi:10.1016/j.agrformet.2018.01.006, 2018.
- 750 Quansah, E., Mauder, M., Balogun, A. A., Amekudzi, L. K., Hingerl, L., Bliefernicht, J. and Kunstmann, H.: Carbon dioxide fluxes from contrasting ecosystems in the Sudanian Savanna in West Africa, *Carbon Balance Manag.*, 10(1), 1–17, doi:10.1186/s13021-014-0011-4, 2015.
- Rannik, Ü., Altimir, N., Raittila, J., Suni, T., Gaman, A., Hussein, T., Hölttä, T., Lassila, H., Latokartano, M., Lauri, A., Natsheh, A., Petäjä, T., Sorjamaa, R., Ylä-Mella, H., Keronen, P., Berninger, F., Vesala, T., Hari, P. and Kulmala, M.: Fluxes 755 of carbon dioxide and water vapour over Scots pine forest and clearing, *Agric. For. Meteorol.*, 111(3), 187–202, doi:10.1016/S0168-1923(02)00022-9, 2002.
- Räsänen, M., Aurela, M., Vakkari, V., Beukes, J. P., Zyl, P. G. Van, Josipovic, M., Venter, A. D., Jaars, K., Siebert, S. J., Laurila, T., Tuovinen, J. and Laakso, L.: Carbon balance of a grazed savanna grassland ecosystem in South Africa, , (July), 1–27, doi:10.5194/bg-2016-268, 2016.
- 760 Räsänen, M., Aurela, M., Vakkari, V., Beukes, J. P., Tuovinen, J. P., Van Zyl, P. G., Josipovic, M., Venter, A. D., Jaars, K., Siebert, S. J., Laurila, T., Rinne, J. and Laakso, L.: Carbon balance of a grazed savanna grassland ecosystem in South Africa, *Biogeosciences*, 14(5), 1039–1054, doi:10.5194/bg-14-1039-2017, 2017.
- Reichstein, M., Falge, E., Baldocchi, D., Papale, D., Aubinet, M., Berbigier, P., Bernhofer, C., Buchmann, N., Gilmanov, T., Granier, A., Grünwald, T., Havránková, K., Ilvesniemi, H., Janous, D., Knohl, A., Laurila, T., Lohila, A., Loustau, D., 765 Matteucci, G., Meyers, T., Miglietta, F., Ourcival, J. M., Pumpanen, J., Rambal, S., Rotenberg, E., Sanz, M., Tenhunen, J., Seufert, G., Vaccari, F., Vesala, T., Yakir, D. and Valentini, R.: On the separation of net ecosystem exchange into assimilation and ecosystem respiration: Review and improved algorithm, *Glob. Chang. Biol.*, 11(9), 1424–1439, doi:10.1111/j.1365-2486.2005.001002.x, 2005.



- 770 Reyers, B., O'Farrell, P. J., Cowling, R. M., Egoh, B. N., le Maitre, D. C. and Vlok, J. H. J.: Ecosystem services, land-cover change, and stakeholders: Finding a sustainable foothold for a semiarid biodiversity hotspot, *Ecol. Soc.*, 14(1), doi:10.5751/ES-02867-140138, 2009.
- Richardson, A. D., Aubinet, M., Barr, A. G., Hollinger, D. Y., Ibrom, A., Lasslop, G. and Reichstein, M.: Uncertainty Quantification, in *Eddy Covariance*, pp. 173–209., 2012.
- 775 Richter, D. and Houghton, R. A.: Gross CO₂ fluxes from land-use change: Implications for reducing global emissions and increasing sinks, *Carbon Manag.*, 2(1), 41–47, doi:10.4155/cmt.10.43, 2011.
- Rogiers, N.: Impact of site history and land-management on CO₂ fluxes at a grassland in the Swiss Pre-Alps, Universität Bern., 2005.
- Roux, P.: Complete inventory of the Camp No.6 veld grazing experiment. (Middelburg, Eastern Cape)., Grootfontein Agric. Dev. Inst. Arch., 1993.
- 780 Schmid, H. P.: Footprint modeling for vegetation atmosphere exchange studies: A review and perspective, *Agric. For. Meteorol.*, 113(1–4), 159–183, doi:10.1016/S0168-1923(02)00107-7, 2002.
- Scott, R. L., Hamerlynck, E. P., Jenerette, G. D., Moran, M. S. and Gafford, G. A. B.: Carbon dioxide exchange in a semidesert grassland through drought - induced vegetation change, *J. Geophys. Res.*, 115(G03026), 1–12, doi:10.1029/2010JG001348, 2010.
- 785 Seymour, C. L., Milton, S. J., Joseph, G. S., Dean, W. R. J., Dithobolo, T. and Cumming, G. S.: Twenty years of rest returns grazing potential, but not palatable plant diversity, to Karoo rangeland, South Africa, *J. Appl. Ecol.*, 47(4), 859–867, doi:10.1111/j.1365-2664.2010.01833.x, 2010.
- Song-Miao Fan, Wofsy, S. C., Bakwin, P. S., Jacob, D. J. and Fitzjarrald, D. R.: Atmosphere-biosphere exchange of CO₂ and O₃ in the central Amazon forest, *J. Geophys. Res.*, 95(D10), 16, doi:10.1029/jd095id10p16851, 1990.
- 790 Sorokin, Y., Zelikova, T. J., Blumenthal, D., Williams, D. G. and Pendall, E.: Seasonally contrasting responses of evapotranspiration to warming and elevated CO₂ in a semiarid grassland, *Ecohydrology*, 10(7), 1–12, doi:10.1002/eco.1880, 2017.
- 795 Sun, D. S., Wesche, K., Chen, D. D., Zhang, S. H., Wu, G. L., Du, G. Z. and Comerford, N. B.: Grazing depresses soil carbon storage through changing plant biomass and composition in a Tibetan alpine meadow, *Plant, Soil Environ.*, 57(6), 271–278, doi:10.17221/7/2011-pse, 2011.
- Tagesson, T., Fensholt, R., Cropley, F., Guiro, I., Horion, S., Ehammer, A. and Ardö, J.: Dynamics in carbon exchange fluxes for a grazed semi-arid savanna ecosystem in West Africa, *Agric. Ecosyst. Environ.*, 205, 15–24, doi:10.1016/j.agee.2015.02.017, 2015.



- 800 Tagesson, T., Ardö, J., Guiro, I., Cropley, F., Mbow, C., Horion, S., Ehammer, A., Mougín, E., Delon, C., Galy-Lacaux, C. and Fensholt, R.: Very high CO₂ exchange fluxes at the peak of the rainy season in a West African grazed semi-arid savanna ecosystem, *Geogr. Tidsskr. - Danish J. Geogr.*, 116(2), 93–109, doi:10.1080/00167223.2016.1178072, 2016.
- Talore, D. G., Tesfamariam, E. H., Hassen, A., Du Toit, J. C. O., Klampp, K. and Jean-Francois, S.: Long-term impacts of grazing intensity on soil carbon sequestration and selected soil properties in the arid Eastern Cape, South Africa, *J. Sci. Food Agric.*, 96(6), 1945–1952, doi:10.1002/jsfa.7302, 2016.
- 805 du Toit, G. van N., Snyman, H. A. and Malan, P. J.: Physical impact of sheep grazing on arid Karoo subshrub/grass rangeland, South Africa, *South African J. Anim. Sci.*, 41(3), 280–287, doi:10.4314/sajas.v41i3.11, 2011.
- du Toit, J. C. O. and Nengwenani, T. P.: [Boesmanskop compositional data 2007-2019]. Unpublished data, 2019.
- du Toit, J. C. O. and O'Connor, T. G.: Changes in rainfall pattern in the eastern Karoo, South Africa, over the past 123 years, *Water SA*, 40(3), 453–460, doi:10.4314/wsa.v40i3.8, 2014.
- 810 du Toit, J. C. O. and O'Connor, T. G.: Long-term influence of season of grazing and rainfall on vegetation in the eastern Karoo, South Africa, *African J. Range Forage Sci.*, 37(2), 159–171, doi:10.2989/10220119.2020.1725122, 2020.
- du Toit, J. C. O., van den Berg, L. and O'Connor, T. G.: Fire effects on vegetation in a grassy dwarf shrubland at a site in the eastern Karoo, South Africa, *African J. Range Forage Sci.*, 32(1), 13–20, doi:10.2989/10220119.2014.913077, 2015.
- du Toit, P. C. V.: Boesmanskop grazing-capacity benchmark for the Nama-Karoo, *Grootfontein Agric*, 5, 1–6, 2002.
- 815 Twine, T. E., Kustas, W. P., Norman, J. M., Cook, D. R., Houser, P. R., Meyers, T. P., Prueger, J. H., Starks, P. J. and Wesely, M. L.: Correcting eddy-covariance flux underestimates over a grassland, *Agric. For. Meteorol.*, 103(3), 279–300, doi:10.1016/S0168-1923(00)00123-4, 2000.
- Valentini, R., Arneth, A., Bombelli, A., Castaldi, S., Cazzolla Gatti, R., Chevallier, F., Ciais, P., Grieco, E., Hartmann, J., Henry, M., Houghton, R. A., Jung, M., Kutsch, W. L., Malhi, Y., Mayorga, E., Merbold, L., Murray-Tortarolo, G., Papale, D., 820 Peylin, P., Poulter, B., Raymond, P. A., Santini, M., Sitch, S., Vaglio Laurin, G., Van Der Werf, G. R., Williams, C. A. and Scholes, R. J.: A full greenhouse gases budget of africa: Synthesis, uncertainties, and vulnerabilities, *Biogeosciences*, 11(2), 381–407, doi:10.5194/bg-11-381-2014, 2014.
- Veenendaal, E. M., Kolle, O. and Lloyd, J.: Seasonal variation in energy fluxes and carbon dioxide exchange for a broad-leaved semi-arid savanna (Mopane woodland) in Southern Africa, *Glob. Chang. Biol.*, 10, 318–328, doi:10.1046/j.1529- 825 8817.2003.00699.x, 2004.
- Vickers, D. and Mahrt, L.: Quality Control and Flux Sampling Problems for Tower and Aircraft Data, *J. Atmos. Ocean. Technol.*, 14, 512–526, doi:10.1175/1520-0426(1997)014<0512:QCAFSP>2.0.CO;2, 1997.
- Villegas, J. C., Espeleta, J. E., Morrison, C. T., Breshears, D. D. and Huxman, T. E.: Factoring in canopy cover heterogeneity



- on evapotranspiration partitioning: Beyond big-leaf surface homogeneity assumptions, *J. Soil Water Conserv.*, 69(3), 78A-830 83A, doi:10.2489/jswc.69.3.78A, 2014.
- Wagle, P., Gowda, P. H., Northup, B. K., Starks, P. J. and Neel, J. P. S.: Response of tallgrass prairie to management in the U.S. Southern great plains: Site descriptions, management practices, and eddy covariance instrumentation for a Long-Term Experiment, *Remote Sens.*, 11(17), doi:10.3390/rs11171988, 2019.
- Wang, J., Li, Y., Bork, E. W., Richter, G. M., Chen, H.-I. E. C., Shah, S. H. H. and Mezbahuddin, S.: Effects of grazing management on spatio-temporal heterogeneity of soil carbon and greenhouse gas emissions of grasslands and rangelands: 835 monitoring, modelling and upscaling, *J. Chem. Inf. Model.*, 53(9), 1689–1699, doi:10.20944/preprints201907.0003.v1, 2019.
- Wang, L., Liu, H. and Bernhofer, C.: Response of carbon dioxide exchange to grazing intensity over typical steppes in a semi-arid area of Inner Mongolia, *Theor. Appl. Climatol.*, 128(3–4), 719–730, doi:10.1007/s00704-016-1736-7, 2016.
- Webb, E. K., Pearman, G. I. and Leuning, R.: Correction of flux measurements for density effects due to heat and water vapour 840 transfer, *Q. J. R. Meteorol. Soc.*, 106(447), 85–100, doi:10.1002/qj.49710644707, 1980.
- Wilczak, J. M., Oncley, S. P. and Stage, S. A.: Sonic anemometer tilt correction algorithms, *Boundary-Layer Meteorol.*, 99(1), 127–150, doi:10.1023/A:1018966204465, 2001.
- Williams, C. A. and Albertson, J. D.: Contrasting short- and long-timescale effects of vegetation dynamics on water and carbon fluxes in water-limited ecosystems, *Water Resour. Res.*, 41, 1–13, doi:10.1029/2004WR003750, 2005.
- 845 Williams, C. A., Hanan, N., Scholes, R. J. and Kutsch, W.: Complexity in water and carbon dioxide fluxes following rain pulses in an African savanna, *Oecologia*, 161(3), 469–480, doi:10.1007/s00442-009-1405-y, 2009.
- Wutzler, T., Lucas-Moffat, A., Migliavacca, M., Knauer, J., Sickel, K., Šigut, L., Menzer, O. and Reichstein, M.: Basic and extensible post-processing of eddy covariance flux data with REddyProc, *Biogeosciences*, 15(16), 5015–5030, doi:10.5194/bg-15-5015-2018, 2018.
- 850 Xu, L. and Baldocchi, D. D.: Seasonal variation in carbon dioxide exchange over a Mediterranean annual grassland in California, *Agric. For. Meteorol.*, 123(1–2), 79–96, doi:10.1016/j.agrformet.2003.10.004, 2004.
- Yan, D., Scott, R. L., Moore, D. J. P., Biederman, J. A. and Smith, W. K.: Understanding the relationship between vegetation greenness and productivity across dryland ecosystems through the integration of PhenoCam, satellite, and eddy covariance data, *Remote Sens. Environ.*, 223(December 2018), 50–62, doi:10.1016/j.rse.2018.12.029, 2019.
- 855 Yan, R., Tang, H., Xin, X., Chen, B., Murray, P. J., Yan, Y., Wang, X. and Yang, G.: Grazing intensity and driving factors affect soil nitrous oxide fluxes during the growing seasons in the Hulunber meadow steppe of China, *Environ. Res. Lett.*, 11, doi:10.1088/1748-9326/11/5/054004, 2016.
- Yan, R. R., Tang, H. J., Lv, S. H., Jin, D. Y., Xin, X. P., Chen, B. R., Zhang, B. H., Yan, Y. C., Wang, X., Murray, P. J., Yang,



- 860 G. X., Xu, L. J., Li, L. H. and Zhao, S.: Response of ecosystem CO₂ fluxes to grazing intensities- A five-year experiment in the Hulunber meadow steppe of China, *Sci. Rep.*, 7(1), 1–12, doi:10.1038/s41598-017-09855-1, 2017.
- Yepez, E. and Williams, D.: Precipitation pulses and ecosystem carbon and water exchange in arid and semi-arid environments, in *Perspectives in Biophysical Plant Ecophysiology: a Tribute to Park S. Nobel*, edited by E. De la Barrera and W. K. Smith, pp. 337–361., 2009.
- 865 Yi, C., Rustic, G., Xu, X., Wang, J., Dookie, A., Wei, S., Hendrey, G., Ricciuto, D., Meyers, T., Nagy, Z. and Pinter, K.: Climate extremes and grassland potential productivity, *Environ. Res. Lett.*, 7(3), 6, doi:10.1088/1748-9326/7/3/035703, 2012.
- Zhou, Y., Pei, Z., Su, J., Zhang, J., Zheng, Y., Ni, J., Xiao, C. and Wang, R.: Comparing soil organic carbon dynamics in perennial grasses and shrubs in a saline-alkaline arid region, northwestern china, *PLoS One*, 7(8), doi:10.1371/journal.pone.0042927, 2012.
- 870 Ziervogel, G., New, M., Archer van Garderen, E., Midgley, G., Taylor, A., Hamann, R., Stuart-Hill, S., Myers, J. and Warburton, M.: Climate change impacts and adaptation in South Africa, *Wiley Interdiscip. Rev. Clim. Chang.*, 5(5), 605–620, doi:10.1002/wcc.295, 2014.